Franz Mlynek, BSc

# SEPARATION OF SILVER NANOPARTICLES FROM IONIC SILVER WITH HPLC-ICPMS

**MASTER'S THESIS**

to achieve the university degree of

Master of Science

Master's degree programme: Environmental Systems Sciences/Natural Sciences - Technology

submitted to

**Graz University of Technology**

Supervisor

Ao.Univ.-Prof. Mag. Dr.rer.nat. Walter Gössler

Institute for Chemistry - Analytical Chemistry
University of Graz

Graz, December 2015

## AFFIDAVIT

I declare that I have authored this thesis independently, that I have not used other than the declared sources/resources, and that I have explicitly indicated all material which has been quoted either literally or by content from the sources used. The text document uploaded to TUGRAZonline is identical to the present master‘s thesis dissertation.

23.12.2015

Date

Signature

*The important thing is to not stop questioning.*
*Curiosity has its own reason for existing.*

**Albert Einstein (1879 - 1955)**

## Abstract

Nowadays, silver nanoparticles (AgNPs) are used in various consumer products because of their antibacterial effect. Due to the widespread use of these products lots of AgNPs are released into our environment. Investigations have shown that AgNPs are less toxic than ionic silver. However, several studies indicate that AgNPs can have a toxic effect on the aquatic ecosystem because of their slow release of ionic silver. Therefore, a fast and robust separation method which is able to differentiate between AgNPs and ionic silver is needed. The goal of this work was the development and optimization of an HPLC-ICPMS method using either a size exclusion column (SEC) or a reversed-phase (RP) column that allows the reliable chromatographic separation of ionic silver from AgNPs.

Prior to the measurements the stability of the silver concentration in the measurement solutions was investigated over 4, 8 and 24 hours. Therefore, different coated AgNPs were stored at different concentrations either in glass or polypropylene (PP) tubes, which were either diluted with ultrapure water or buffer solution. The highest stability was observed for storage in buffer solution and PP as storage container material.

A published liquid chromatographic method using a RP-column for the separation of ionic silver from citrate-AgNPs served as starting point. One of the separation mechanisms was explained to be a size-exclusion effect. Therefore, a size-exclusion column was used in this work. First results looked quite promising, but the reproducibility was not satisfying, because of an increasing citrate-AgNP signal within consecutive injections of the same sample. It was not possible to find an explanation for this effect and even when the conditions were changed to the original method the problem could not be solved.

Right now the method is quite good for a qualitative determination of ionic silver and AgNPs in an unknown sample. But for quantitative analysis there is still some work to do.

## Zusammenfassung

Heutzutage werden Silbernanopartikel (AgNP) in verschiedensten Konsumgütern aufgrund ihrer antibakteriellen Wirkung eingesetzt. Wegen ihres weitverbreiteten Einsatzes gelangen sie schlussendlich auch in die Umwelt. Studien haben gezeigt, dass Silbernanopartikel eine geringere Toxizität als ionisches Silber aufweisen. Jedoch können Silbernanopartikel eine toxische Wirkung auf das aquatische Ökosystem haben, da sie langsam aber stetig Silberionen freisetzen. Daher besteht der Bedarf an einer schnellen und robusten Analysenmethode, mit welcher man Silberionen von Silbernanopartikeln unterscheiden kann. Das Ziel dieser Arbeit war die Entwicklung und Optimierung einer HPLC-ICPMS Methode, die mit Hilfe einer Größenausschlusssäule oder einer Umkehrphasen-Säule (RP) die zuverlässige Trennung von Silberionen von AgNPs ermöglicht.

Vor den eigentlichen Messungen wurde die Stabilität der Silberkonzentration in den Messlösungen überprüft. Hierfür wurden unterschiedlich modifizierte AgNPs für 4, 8 und 24 Stunden bei unterschiedlichen Konzentrationen gelagert. Als Gefäßmaterial wurde entweder Glas oder Polypropylen (PP) verwendet. Die Proben wurden entweder mit hochreinem Wasser oder Puffer verdünnt. Die größte Stabilität wurde bei mit Puffer verdünnten AgNPs in PP-Gefäßen beobachtet.

Der Startpunkt dieser Arbeit war eine veröffentliche Methode zur Trennung von Silberionen und Citrat-AgNPs mittels einer RP-Säule. Es wird angenommen, dass einer der Trennmechanismen auf dem Größenausschlussprinzip basiert. Aus diesem Grund wurden die Trennungen in dieser Arbeit mit einer Größenausschlusssäule durchgeführt. Jedoch war bei einer Mehrfachinjektion von ein und derselben Probe ein Anstieg des AgNP-Signals zu beobachten.

Bisher konnte noch kein Grund für die schlechte Reproduzierbarkeit der Messungen gefunden werden. Zurzeit ist die Methode daher nur für die qualitative Bestimmung von ionischem Silber und AgNPs in einer unbekannten Probe geeignet.

## Acknowledgements

Ich möchte dir, **Walter**, recht herzlich danken, dass ich meine Masterarbeit bei dir schreiben durfte und in den vergangen 2 Jahren einiges von dir lernen konnte. Sei es die Betreuung von Studenten, das Reparieren von Geräten, das Finden von Lösungen für diverse analytische Probleme oder das kritische Hinterfragen von Analyseergebnissen und wissenschaftlichen Arbeiten. Vielen Dank vor allem für die Möglichkeit im letzten halben Jahr an diversen Projekten mitwirken zu dürfen, die meinen wissenschaftlichen Horizont enorm erweitert haben. Zuletzt herzlichen Dank für die Biersprechungen und die tollen Ausflüge auf die Hütte im Lachtal.

Großer Dank gebührt vor allem meiner Familie - **Mama**, **Alex** und **Georg**. Dafür, dass ihr immer für mich da seid, mich in schwierigen Phasen und bei der Verwirklichung meiner Ziele immer unterstützt. Danke **Kristin**, **Verena**, **Oma** und **Opa,** dass ihr auch immer für mich da seid. Natürlich auch ein Danke an **Simon** und **Mia**, dass ihr mich beim Babysitten auf Trab haltet und so oft zum Lachen bringt.

Vielen Dank dem Bereich analytische Chemie und vor allem dem gesamten **ACHE**-Team, dass ihr mir mit Rat und Tat zur Seite gestanden seid. Ich weiß, dass es manchmal mühsam war, mein Gejammere wegen einer missglückten Messung ertragen zu müssen. Ein besonderer Dank gilt natürlich **Chris**, der mich einen großen Teil meines Studiums begleitet hat und ein toller Lern- und Biersprechungskollege war. Auch **Lisa**, **Oli**, **Stefan** und **Anja** - ihr seid mit der Zeit abgesehen von Arbeitskollegen auch tolle Freunde geworden - Danke dafür. Danke **Fripi** für die unterhaltsamen Mittags- und Kaffeepausen. Danke auch an **Jaqui** und **Hanna** für die Hilfe bei der Vorbereitung meiner Messungen.

Danke **Alex** und **Geri**, dass ihr so tolle Freunde seid und es immer toll ist Zeit mit euch zu verbringen. Sei es auf einem Surftrip oder auch nur bei einem gemütlichen Bier in Graz oder Linz. Auch wenn wir uns mal länger nicht sehen,

weiß ich trotzdem immer, dass auf euch Verlass ist. Danke natürlich auch der restlichen "**Pfadirunde**".

**David**, **Gabriel**, **Matthias**, **Sili** & **Hari** – ihr seid einfach die Besten. Es ist immer wieder wie Urlaub Zeit mit euch zu verbringen, weil ich einfach abschalten und die Zeit genießen kann. Sei es beim Wakeboarden, bei einem legendären Roadtrip nach Spanien, beim Mountainbiken und Beachen oder einfach beim Bierchen genießen. Danke natürlich auch der restlichen "**Schneiderrunde**".

Vielen Dank an **Prof. Otto Glatter** für die Möglichkeit, DLS-Messungen durchführen zu können. Danke auch an **Franz Pirolt** für die Unterstützung bei der Durchführung der Messungen.

Herzlichen Dank an **Ivana Vinković Vrček** für die Bereitstellung deiner Synthesevorschriften, der Zurverfügungstellung diverser Silbernanopartikel Lösungen sowie die dafür durchgeführten DLS Messungen.

# 1 Introduction

## 1.1 Silver

Silver (Ag) is a noble metal. It occurs naturally in its pure form or bound as sulfide in sulfide silver ores or silver containing ores. The natural isotopes are $^{107}Ag$ (51.83 %) and $^{109}Ag$ (48.17 %). [1]

In the review of Russell and Hugo it was mentioned that silver has already been used in various forms for a long time. Around 3500 BC silver was used as currency in Egypt. Since 1000 BC or probably before it was known that water could be kept drinkable, when it was stored in copper or silver vessels. At the end of the 19$^{th}$ century it was known that very low silver concentrations have an antimicrobial effect. Therefore silver was used to prevent eye infections in newborn. At the beginning of the 20$^{th}$ century it was discovered in various experiments that pure silver doesn't have an antimicrobial activity. That's why it was suspected that oxidized silver releases $Ag^+$ ions, which are responsible for the antimicrobial action. [2]

## 1.2 Antibacterial mechanism of silver

**Disruption of cell membrane.** Silver ions interact with the peptidoglycan cell wall and cause lysis of the membrane. [3]

**DNA binding.** Silver ions bind to the DNA, the DNA condenses and loses its replication ability, what results in the prevention of bacterial reproduction. [3]

**Respiration blocking**. Silver blocks the respiration and the electron transfer of bacteria by reacting with sulfhydryl groups (-SH) on the surface of the bacteria. There are two possibilities on how the silver reacts with the sulfhydryl groups. In one possibility the silver has oxygen adsorbed on its surface, the oxygen reacts with the hydrogen atoms of pairs of sulfhydryl groups and form R-S-S-R bonds under the loss of water. The second possibility is that the silver ions react directly with the sulfhydryl group, which results in a stable –S-Ag bond. [4]

**Irreversible Inhibition of Enzymes**. $Ag^+$ is able to irreversibly inhibit enzymes by reacting with essential sulfhydryl groups. The mercaptides are formed like this: Enz-SH + $Ag^+$ → Enz-S-Ag + $H^+$. [5]

## 1.3 Antibacterial activity of silver

As mentioned before the antibacterial activity of silver has been known for a long time. For a better understanding of the antibacterial activity several model organisms are exposed to various silver compounds and the effects on them and the morphological changes of them are observed. Below several studies concerning the antibacterial activity of silver are listed.

Feng and co-workers investigated the effect of $AgNO_3$ on the *E. coli* (ATCC 23282) and the *S. aureus* (ATCC 35696) bacteria. The observed phenomena which are similar for both types of bacteria are: in the center of the cells an electron-light region appeared, in the center of the electron-light region were some condensed substances (these might be a condensed form of DNA molecules, because in the condensed substances a large amount of phosphorous was present), between the cell wall and the cytoplasm membrane a big gap existed and silver was present in the cytoplasm. But there were also some minor differences between the two bacteria types: the *S. aureaus* bacteria remained intact, there was a smaller amount of electron-dense granules inside the cells and compared to the *E. coli* bacteria, the electron-light region was darker. [6]

The antibacterial activity of an ionic silver solution, which was electrically generated in a washing machine, was investigated by Jung and co-workers. *S. aureus* and *E. coli* bacteria were successfully removed from a contaminated fabric in a washing cycle. It is unknown whether the bacteria were removed just because of the washing cycle or killed by the silver ions. They further did conventional plate counting tests with this ionic silver solution. The number of *S. aureus* bacteria was significantly reduced after 90 minutes and the *E. coli* bacteria were already eliminated after 30 minutes of treatment. They also observed morphological changes in these two bacteria types. *S. aureus* and *E. coli* cells underwent lysis and became disrupted. They released their cellular contents into the ambient environment due to broken cell walls and cytoplasm membranes. Electron-dense particles and precipitates were thereby released

and found around the damaged bacterial cells. Further the cell membrane was locally or completely detached from the shrank cytoplasm membrane. [7]

Klueh and co-workers showed in batch- and flowing-fluid experiments that the growth rate of *Staphylococcus epidermidis* on poly(ethylene terephthalate) fabrics is reduced up to 6 times when they are coated with silver. The silver is attached on the fabric via ion beam assisted deposition (IBAD). [8]

### 1.4 Definition of nanoparticles

According to the European Commission Recommendation (2011/696/EU) the term “Nanomaterial” means: “*A natural, incidental or manufactured material containing particles, in an unbound state or as an aggregate or as an agglomerate and where, for 50 % or more of the particles in the number size distribution, one or more external dimensions is in the size range 1 nm - 100 nm.”* [9]

### 1.5 Silver nanoparticles in consumer products

Nowadays many consumer products contain silver nanoparticles because of their antibacterial effects. The list below shows a few examples [10]:

**Household products**: washing machines, refrigerators, air conditioners, microwave ovens, vacuum cleaners, dehumidifiers, water dispensers, air purifiers.

**Kitchen products**: fruit juicers, plastic food containers, cutting boards, wraps for food, pots, dishes.

**Baby products**: baby bottles, wet tissues.

**Bathroom products**: toothpaste, toilet lid, toothbrushes, soaps, shampoo, hair supplies.

**Textiles**: underwear, socks, shoes.

**Various other products**: computer appliances, cellular phones, medical products, hygiene products, parquet, door handles, doors.

## 1.6 Toxicity of silver nanoparticles

Whether or not AgNPs are toxic on its own or just because of its release of $Ag^+$ ions or due to the combination of both or aren't toxic at all is the subject of many studies with various model organisms. Several studies and their results are listed below.

Verano-Braga and co-workers used human colon carcinoma cell line (LoVo) as an in vitro model. They investigated the effect of 20 nm and 100 nm citrate(cit)-AgNPs on these cells. 467 proteins were differentially regulated due to the exposure to 20 nm cit-AgNPs and 306 when exposed to 100 nm particles. They observed that mitochondrial proteins showed a trend to be more down-regulated than up-regulated whereas cytosolic proteins had the opposite tendency. They concluded that cellular oxidative stress is induced due to the exposure to 20 nm AgNPs and to a lesser extent by 100 nm AgNPs. This causes DNA damage, apoptosis and protein damage which leads to ubiquitination and degradation through proteasomes. Further the mitochondrial activity is reduced as a result of the down-regulation of proteins which are involved in the electron transport chain. Finally they showed that there is a size dependent cellular uptake of the AgNPs by the means of confocal laser scanning microscopy of the LoVo cells. They stated that 20 nm AgNPs penetrated the cells and large clusters of aggregated AgNPs were found inside the cells. They further observed morphological changes in the LoVo cells like rounded shapes which are an indication of cellular stress. On the other hand only a few 100 nm AgNPs were assimilated by the LoVo cells. The majority of the nanoparticles were located on the plasma membrane. [11]

Loeschner and co-workers observed the effect of 14 nm polyvinylpyrrolidone(PVP)-AgNPs and silver acetate (AgAc) on female Wistar Hannover Galas rats after repeated oral intake. The rats were fed twice a day for 28 days. The silver distribution pattern in the organs was quite similar regardless of PVP-AgNP or AgAc exposure. Silver was found in following organs (listed from highest to lowest Ag concentration): small intestine, stomach, liver, kidney, lungs, muscle, brain and plasma. Therefore the organs

were either digested with nitric acid and analyzed with ICPMS or analyzed with autometallographic staining (AMG). It is interesting to see that the silver concentration in the organs of rats exposed to PVP-AgNPs was at least 40 % up to 90 % lower than those exposed to AgAc. They presume that this difference might be because of the higher excretion of silver in feces after oral intake of PVP-AgNPs. They further claim that there were no AgNPs present in the feces. Therefore dried feces were analyzed with scanning electron microscopy (SEM) and an aqueous extract of the feces was analyzed with transmission electron microscopy (TEM). Yet they suggest that further experiments are needed to substantiate this statement. It is also fascinating that there is nearly no silver (<0.1 %) excreted in urine independent of the silver source. Finally they recommended that further investigation will be necessary to figure out if the whole AgNP is absorbed or whether it is dissolved in the gastrointestinal system and redeposited in the tissue. [12]

Ribeiro and co-workers used either NanoSilver Hx or NanoSilver OP 1000 from AMEPOX (Poland) and $AgNO_3$ as silver sources. The NanoSilver solution consists of nanosized silver dispersed in paraffin chemical oils, but the exact AgNP type couldn't be found in theirs work. For the microalgae *Pseudokirchneriella subcapitata* the growth rate is reduced more by AgNPs than by $AgNO_3$ except for a mid-level concentration, where $AgNO_3$ reduces the growth rate more than AgNPs. The reproduction rate of *Daphnia magna* is already reduced at very low $AgNO_3$ concentrations, but for AgNPs the rate is reduced only at slightly higher concentrations. The growth is not significantly affected by any of them. The hatching rate of the zebrafish *Danio rerio* was reduced more by $AgNO_3$ compared to the same concentration of AgNPs. Further the zebrafish embryos also had developmental abnormalities already at lower $AgNO_3$ concentration in contrast to the AgNPs. [13]

Choi and co-workers used nitrifying bacteria and *E. coli* PHL628-gfp as model organisms. They observed the effects of $AgNO_3$, 14 nm polyvinyl alcohol(PVA)-AgNPs and AgCl colloids on these two bacteria types. AgNPs inhibited the growth of nitrifying bacteria at nearly 90 % whereas the inhibition with $AgNO_3$ and AgCl was just between 40 – 50 %. For *E. coli* on the other hand $AgNO_3$

was most toxic. The growth was inhibited by 100 % whereas AgCl reduced growth by 66 % and AgNPs by 55 %. Further it is remarkable that AgCl has a toxic effect at all which is even in the same magnitude as PVA-AgNPs and $AgNO_3$ regarding the bacteria type. [14]

Xiu and co-workers investigated the effects of carbon coated silver nanopowder and $AgNO_3$ on *E. coli* strain K12 (ATCC 25404) bacteria. The *E. coli* mortality after 6 h $AgNO_3$ exposure was nearly 100 % both under aerobic and anaerobic conditions. Reactive oxygen species (ROS) induced oxidative stress is suspected to be one antibacterial mechanism for silver ions. Due to the reason that ROS can't be produced in a sufficient amount in an anaerobic environment other mechanisms like the inactivation of thiol-containing proteins should play a bigger role in the antibacterial effect of silver. They also investigated that AgNPs were 20 times less toxic than $AgNO_3$ under anaerobic conditions but after exposure to air for half an hour their toxicity increased 2.3-fold. This is due to the release of $Ag^+$ from the surface of the AgNPs. [15]

Sotiriou and Pratsinis investigated the antibacterial activity of $Ag/SiO_2$ nanoparticles on *E. coli* (JM101) bacteria. They showed that the smaller the particles are, the higher the concentration of released $Ag^+$ ions is because of the higher volume to surface ratio of the particles. This results in a higher antibacterial activity. For larger $Ag/SiO_2$ nanoparticles the *E. coli* growth is only prevented at higher particle concentrations. They conclude that the antibacterial activity is just because of the release of $Ag^+$ ions. [16]

Xiu and co-workers studied the toxicity of 5 and 11 nm polyethylene glycol(PEG)-AgNPs on *E. coli* strain K12 (ATCC 25404) bacteria. They exposed the *E. coli* bacteria to AgNPs under anaerobic conditions. They showed that no silver ions were released and that the bacteria stayed alive. Under aerobic conditions $Ag^+$ ions were released and the bacteria were killed. They conclude that AgNP toxicity is only because of $Ag^+$ release due to oxidation of the silver core and that the particles themself have no effect on the bacteria. They further investigated that the AgNP toxicity is size depend. The reason for this is that the

smaller the particles are, the higher the particle volume:surface ratio is and the higher the $Ag^+$ release is because of the oxidation of the AgNPs. [17]

Lok and co-workers used fully reduced 9 nm cit-AgNPs, surface oxidized 9 and 60 nm cit-AgNPs and $AgNO_3$ for their experiments. They assumed that the fully reduced cit-AgNPs, which were synthesized and stored under a nitrogen atmosphere, don't release any $Ag^+$ ions under anaerobic conditions. Surface oxidized cit-AgNPs have $Ag^+$ ions adsorbed on their surface, which can be easily released. Therefore oxygen was bubbled through a cit-AgNP solution for 30 minutes. *E. coli* strain (K12, MG1655) and the silver-resistant strains 116$AgNO_3$R and J53 (pMG101) were chosen as their test organisms. They investigated that the fully reduced AgNPs didn't affect the *E. coli* colony formation. Also when the $Ag^+$ ions on the surface of the 9 nm surface oxidized AgNPs were reduced to $Ag^0$ with borohydride, the AgNPs had no effect on the growth of the *E. coli.* However, the 9 nm surface oxidized AgNPs showed the same effect as the $AgNO_3$ solution and reduced the *E. coli* colony formation over 90 %. This can be attributed to the silver ions which are present in both solutions. Further they showed that smaller AgNPs (9 nm) are much more antibacterial than bigger ones (62 nm). Only when the AgNP concentration of the 62 nm AgNPs was 9 times higher than that of the smaller ones they showed the same antibacterial activity. The growth of the silver resistant bacteria wasn't affected at all by the surface oxidized AgNPs and $AgNO_3$. [18]

Morones and co-workers investigated the effect of 1 – 100 nm AgNPs inside a carbon matrix on *E. coli*, *V. cholerae*, *P. aeruginosa* and *S. typhus* bacteria. They observed that *P. aeruginosa* and *V. cholera* are more resistant to the particles in contrast to the *E. coli* and *S. typhus* bacteria. Independent of the bacteria type AgNPs were found on the surface of the cell membrane and in the inside of the bacteria. [19]

Sondi and co-workers exposed *E. coli* strain B bacteria to 12 nm Daxad 19-AgNPs. They investigated the growth of the bacteria on agar plates and in liquid LB medium where they observed a significant difference. The growth of *E. coli*

on agar plates was completely inhibited by the AgNPs but in the LB medium the growth was just delayed even at high concentrations. [20]

Lee and co-workers investigated the influence of 12 nm cit-AgNPs on the development of zebrafish embryos. They treated the embryos in the cleavage-stage (8-cells) with various AgNP concentrations. At low AgNP concentrations the percentage of normally developed zebrafish outweighs the dead and deformed ones. As AgNP concentration is slightly increased, the number of dead and deformed zebrafish is increased, whereas the number of normally developed ones is decreased. Beyond a certain AgNP concentration, only dead zebrafish and deformed ones were observed. Following deformities were noticed: finfold abnormality, tail/spinal cord flexure and truncation, cardiac malformation, yolk sac edema, head edema and eye deformity. They further found out that the type of malformation is strongly dependent on the AgNP concentration. [21]

Ahamed and co-workers investigated the influence of polysaccharide coated and uncoated 25 nm AgNPs on mouse embryonic stem (MES) cells and mouse embryonic fibroblasts (MEF). They observed that the uncoated AgNPs agglomerated inside the cell and weren't present in some organelles like the nucleus and the mitochondria. The polysaccharide coated AgNPs didn't agglomerate and were distributed all over the cell. They further noticed that both AgNP types can cause DNA double strand breakage in both investigated cell types. Finally they examined that both AgNP types can induce cell death/apoptosis in both investigated mammalian cell types. [22]

All these studies have shown, that it is not that simple to define to which extent AgNPs are toxic or not. Further it isn't really possible to compare the results of the studies with each other because either AgNPs with different surface coatings were used or different model organisms were investigated or the exposure conditions (aerobic, anaerobic) were different. But the most important factor are the exposure conditions. It is necessary to work under anaerobic conditions because than the impact of released $Ag^+$ ions on the toxic effect can be excluded.

## 1.7 Methods for silver nanoparticle synthesis

There are two approaches to prepare colloidal metal nanoparticles: the “top-down” approach, where bulk metals are subdivided by physical methods and the “bottom-up” approach, where the particle growth starts from metal atoms. [23]

Metal nanoparticles can be prepared for example via “chemical reduction of metal salts”, “laser ablation”, “electrochemical synthesis”, the “plasma method”, “electron beam or γ-irradiation”, the “photochemical method” or via “thermal decomposition methods”. [23, 24]

This work focuses on the “chemical reduction of metal salts as precursors” a “bottom-up” approach. In this method a metal salt, e.g. $AgNO_3$ (silver nitrate), is reduced by a reducing agent, e.g. $NaBH_4$ or citrate, to metal atoms. These free atoms are unstable and quickly nucleate to form metal nanoparticles. This process continuous until a stabilizing agent, e.g. polyvinylpyrrolidone (PVP) or citrate, stops this nucleation and aggregation process and stabilizes the metal nanoparticles. [23, 24]

## 1.8 Stabilization mechanisms of silver nanoparticles

As described above the metal nanoparticles have to be stabilized with a stabilizing agent to prevent agglomeration of the nanoparticles. There are three stabilization mechanisms: (a) steric, (b) electrostatic and (c) electrosteric stabilization (shown in Figure 1).

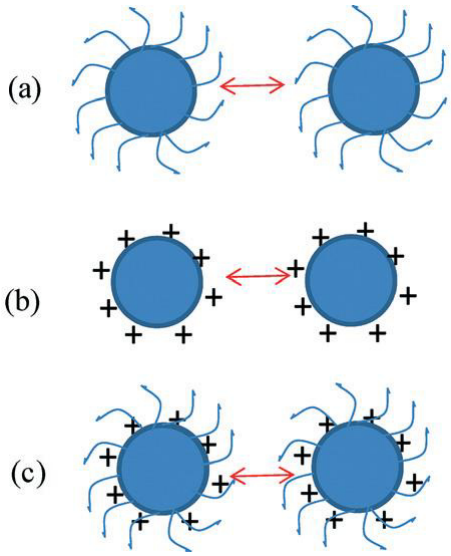


**Figure 1**: Stabilization mechanisms of nanoparticles: (a) steric stabilization, (b) electrostatic stabilization, (c) electrosteric stabilization. Adapted figure from Liu et al. [25].

Steric stabilization is based on the steric repulsion between two neighbouring particles. They have long dangling hydrophilic polymeric chains adsorbed on their surfaces which cause this steric hindrance. [24, 25]

Electrostatic stabilization is due to the repulsive electrostatic force, which the nanoparticles experience from an electrical double layer interaction. The double layer is formed by the accumulation of counter ions near their charged surface. [24, 26]

Electrosteric stabilization is a combination of steric and electrostatic repulsion and is caused by polyelectrolytes. Electrostatic repulsion dominates when the polyelectrolyte adsorbs flat on the particle surface. With an increase of the adsorbed polyelectrolyte layers, the steric repulsion outweighs. [26]

## 1.9 Various detection and characterization techniques for silver nanoparticles

### *1.9.1 Dynamic light scattering (DLS)*

DLS is based on the time-dependent fluctuations of the scattering light intensity. The scattering is caused by the Brownian movement of particles in solution. Hence the diffusion rate can be determined which is then related via the Stokes-Einstein equation to a hydrodynamic diameter. [27]

Filipe and co-workers evaluated the possibilities and limitations of DLS with mono- and polydisperse polystyrene beads. For the monodisperse samples (60 nm, 100 nm, 200 nm, 400 nm, 1000 nm) DLS showed good size accuracy and a narrow distribution, although there was a tailing towards larger sizes. This is due to a few large particles, which contribute a big part to the overall scattering. Next various mixtures of the beads were measured. The mixtures were: 60 nm & 100 nm, 100 nm & 200 nm, 200 nm & 400 nm, 400 nm & 1000 nm. With DLS it wasn't possible to separate any of the two bead sizes of the mixture and measure them accurately. Only one single peak was obtained, which shifted towards the larger of the two particle sizes. Finally a mixture containing 100, 400 and 1000 nm beads was measured. The result was a single peak which could be indicated as a rather monodisperse sample of 700 nm beads. This example shows that such a misinterpretation for a nanoparticle sample can happen quite easily, if it is polydisperse. [28]

### *1.9.2 Nanoparticle tracking analysis (NTA)*

In NTA the properties of Brownian motion and light scattering are utilized. The basic principle of NTA is that a laser beam is scattered by a nanoparticle suspension in a sample chamber. Due to this scattering, the Brownian motion of particles can be easily visualized and captured with a CCD camera. The NTA software calculates the diffusion coefficient from this movement, which can then be related to a hydrodynamic diameter via the Stokes-Einstein equation. [28, 29]

Filipe and co-workers evaluated the strengths and weaknesses of NTA with mono- and polydisperse polystyrene beads. The monodisperse samples (60 nm, 100 nm, 200 nm, 400 nm, 1000 nm) were analyzed with good sizing accuracy and narrow size distribution. Next various mixtures of the beads were measured. The mixtures were: 60 nm & 100 nm, 100 nm & 200 nm, 200 nm & 400 nm, 400 nm & 1000 nm. NTA was able to differentiate the two sizes in all of the mixtures and determine them accurately. Finally a mixture containing 100, 400 and 1000 nm beads was measured. All of the 3 bead sizes could be detected and sized, but the number of the 100 nm decreased by 80 % compared to the nominal value and the 400 nm beads by 35 %. This is due to

the large particles, which have an intense light scattering and therefore it is difficult to detect and track smaller particles. Also the smaller particles move sometimes out of the detection area and thus they can't be tracked long enough for determination. All in all NTA is a good tool to determine the size of mono- and polydisperse particles, although it has some weaknesses in the determination of the number of the particles in polydisperse samples. A big benefit is, that this technique makes the visualization of the particles possible. [28]

### *1.9.3 Transmission electron microscopy (TEM)*

An electron microscope uses a beam of accelerated electrons to image the surface of an object. The theoretical resolution is 0.004 nm for a 100 keV electron. This resolution can't be reached in reality because right now it's not possible to build perfect electron lenses. Thus the effectively image resolution is about 0.1 nm. Therefore it is well suitable for the size characterization of nanoparticles. [30]
With TEM it is possible to get information of the core size of AgNPs. It is not really possible to determine the size of the AgNPs with the organic coating, due to the low contrast of the organic coating in TEM. Further the size distribution obtained with TEM might not be really reliable, because only a few thousand particles are counted and the size distribution is thus strongly dependent on the chosen area. Further the smallest particles might be undercounted, because of their low contrast in TEM. [31]

### *1.9.4 Single particle ICPMS (sp-ICPMS)*

In sp-ICPMS the simultaneous determination of ionic silver and silver nanoparticles in regard to concentration and size distribution is possible. Therefore several thousand intensity readings with dwell times of about 10 ms are continuously monitored. Pulses above the continuous signal, which is caused by dissolved silver, are interpreted as nanoparticle events. The number of events represents the number concentration of the particles in solution. The pulse intensity correlates with the particle size with assumptions such as that

the particle is perfectly rounded or that the particle completely consists of the detected metal. A prerequisite for sp-ICPMS is a low particle number concentration because this limits the possibility that two nanoparticles are detected at the same time which would lead to a falsely determined larger particle. The low particle number concentration is achieved by dilution of the sample. The problem thereby is that a dilution can cause a change in the particle size due to the change of the concentration of the coating compounds. The dilution can further cause dissolution of the particles, which might lead to a higher ionic fraction. Right now the technique is limited to particle sizes not smaller than 20 nm and is further strongly dependent on the signal to noise ratio of the instrument. [32, 33]

Laborda and co-workers investigated with ultrapure water diluted sample solutions of 10, 20, 40, 80 and 113 nm silver nanoparticles and just ionic silver containing samples. For the 113 nm AgNPs they showed the problem of a too high nanoparticle concentration. When the AgNP concentration is too high, then more than one nanoparticle is in the aerosol droplet and the nanoparticle is falsely determined as a bigger nanoparticle, which results in a wrong size distribution. Also if the dwell time is too long, two or more instead of just one particle are detected, which also results in a wrong size distribution. They also showed that the smallest nanoparticle size, which can be determined, is around 20 nm, but if the concentration of ionic silver is high, than the detection limit is even above 30 nm. They further observed that the 10 nm AgNPs can’t be detected, but the presence of these particles can be presumed, with a closer look at the distribution histogram. Ionic silver shows a Poisson distribution, but with the presence of these small particles, the distribution pattern shifts towards a lognormal distribution. Finally they showed that it is possible to resolve the size distribution of a 40 and 80 nm AgNP containing solution. [34]

### *1.9.5 Asymmetrical flow field-flow fractionation (AF4)*

AF4 uses a thin channel which has a semipermeable membrane on the lower side. When the sample is injected, a counter flow is applied to focus the particles at the beginning. After focusing, the counter flow is turned off and only the carrier flow is applied. The carrier flow forms a parabolic flow profile and

carries the particles through the channel. A cross flow results through channeling off a part of the laminar flow through the semipermeable membrane. This cross flow pushes the particles onto the membrane. Through diffusion the smaller particles reach further back into the parabolic flow profile, whereas the larger ones stay closer to the membrane. As a result from the higher flow velocity in the middle of the flow profile, the smaller particles travel faster than the bigger ones. This interaction between the cross flow and the diffusion leads to the separation of the particles of different sizes and as a result smaller particles elute first followed by bigger ones. The ionic fraction is separated through the semipermeable membrane. [35]

Geiss and co-workers used an AF4 system with on-line coupling of an UV-Vis detector at a wavelength of 420 nm and an ICPMS. They determined citrate coated AgNPs in a size range from 10 to 110 nm in 10 nm steps in aqueous solution. They injected each particle size individually to get a calibration curve and used this calibration to quantify particles in a mixture containing 10, 50 and 100 nm AgNPs. The recovery was in the range from 86 % to 106 % depending on the detector. But they also claimed that this is only possible because of perfectly spherical shaped particles used for calibration what doesn't really correspond to real life samples. Further they mentioned that the channel membrane only lasts for about 50 runs and every time it is changed it has to be preconditioned with repeatedly injected AgNPs until a stable UV-Vis signal is observed. Finally they mention some points which have to be noticed when dealing with AF4 separation. The possible interaction between the membrane and the particle depends on the type of particles, the coating of the particles, the composition of the mobile phase and on the membrane material. This might be a problem in reality, because strictly speaking for every particle type a different separation method should be used. Also when dealing with nanoparticles in difficult matrices, the matrix might have an impact on the separation in regard to elution and recovery. [36]

Hoque and co-workers used 10 nm carboxy-functionalized polyacrylate capped AgNPs and 20, 40, 60 and 80 nm uncapped AgNPs for their AF4 experiments. For detection they coupled the AF4 system on-line with an UV-Vis detector at a wavelength of 420 nm or with an ICPMS. They determined the size and the concentration of the AgNPs in aqueous samples. They first showed the

separation of the individually injected uncapped AgNPs with AF4-UV-Vis which showed a nice resolution for the two smaller sizes but a poor one for the two bigger ones. Further a 1:1:1:1 by volume mixture of the uncapped AgNPs was injected. They were just able to separate the 20 nm AgNPs from the other ones. The 80 nm particles weren't detected at all because of the dilution of the sample. This is also due to the compromise of the 420 nm wavelength of the UV-Vis detector mentioned by Geiss et al. [36] which has the highest sensitivity for smaller particles. They didn't use the ICPMS as detector for this mixture or the individual AgNPs. The 10 nm AgNPs were analyzed with an ICPMS as an on-line detector and showed a nice resolution. This system was also used to detect AgNPs in an untreated wastewater sample. Due to a AgNP peak both in an unspiked and a spiked wastewater sample the presence of Ag containing nanosized particles is confirmed. They didn't use the UV-Vis detector for analysis of these samples. [37]

### *1.9.6 Centrifugal field-flow fractionation (CF3)*

In CF3 a ring shaped channel filled with mobile phase is rotated with up to 4900 rpm. Thereby a centrifugal field is generated which forces the particles to the outer wall of the channel. The heavier/larger particles are pressed closer to the outer wall and stay in the slower stream lines of the parabolic flow profile of the mobile phase. The smaller/lighter particles on the other hand stay further away from the outer wall and travel in the faster stream lines. Out of it results, that the smaller particles elute first followed by bigger ones. The ionic fraction normally should elute with the dead time. [35]

Cascio and co-workers investigated 10 nm, 20 nm, 30 nm, 40 nm, 60 nm, 70 nm and 100 nm citrate stabilized silver nanoparticles with CF3-UV-Vis at 420 nm. All samples were injected individually and seem to be monodisperse, except for the 60 nm AgNPs, which show secondary peaks between 70 and 110 nm. This might be because of the different shapes of the AgNPs, what could be observed with TEM. Further two mixtures were investigated, one containing 40 and 60 nm AgNPs (Mix A) and the second 40 and 70 nm AgNPs (Mix B). The two sizes in Mix A could be separated with a resolution of 0.51 and in Mix B with a resolution of 0.89. Unfortunately they didn't use an ICPMS as

detector instead or additionally to the UV-Vis detector, like they did with an AF4 in the same study. [38]

### *1.9.7 RP-HPLC-ICPMS*

In this technique an HPLC system with a RP-column and an ICPMS as detector is used.
Soto-Alvaredo and co-workers separated 10, 20 and 40 nm citrate AgNPs from ionic silver with a 1000 Å C18 column. The smallest AgNPs they were able to separate from ionic silver were about 2 – 3 nm in diameter. Finally they extracted a solution from silver containing sport socks. Therein they found 20 – 40 nm AgNPs, 7 nm AgNPs and ionic silver. [39]

### *1.9.8 Cloud point extraction (CPE)*

In CPE surface-active non-ionic agents like Triton X-114 or Triton X-100 are used. They consist of two parts: a hydrophilic one (polar or ionic headgroup) and a hydrophobic one (hydrocarbon tail). If their concentration exceeds a certain threshold in an aqueous solution, the so called critical micellar concentration, micelles are spontaneously formed. The hydrocarbon tails are orientated to the center of the micelle, forming a hydrophobic core, in which the desired hydrophobic compound can be enclosed. If the micellar solution is heated above a certain temperature, the so called cloud point, it separates into two phases and gets turbid. After a suitable equilibration time at a temperature above the cloud point, the solution is then centrifuged and a surfactant-rich phase forms. To remove the supernatant from the surfactant-rich phase, the tubes are cooled in an ice bath, whereby the viscosity of the surfactant-rich phase increases and the supernatant can just be decanted. In terms of a reproducibly CPE procedure, many parameters have to be considered: temperature, surfactant type and concentration, pH, ionic strength, equilibration time and centrifugation time. [40, 41]
Chao and co-workers used Triton X-114 to separate PVP-AgNPs from ionic silver. They determined the AgNP concentration of the Triton X-114 rich phase with ICPMS after a microwave digestion. Further the total Ag content in the

sample was determined with ICPMS after microwave digestion of the sample. The ionic silver content in the sample was gotten by the difference of the total Ag concentration and the PVP-AgNP concentration of the sample. They conclude that CPE is an efficient method for the speciation of AgNPs and ionic silver. But it might be possible that also other silver species and small amounts of ionic silver might be extracted in the Triton X-114 rich phase and falsely determined as AgNPs. As a consequence they suggest further investigation of the samples with TEM, SEM-EDS and UV-vis. [42]

### *1.9.9 Hydrodynamic chromatography coupled to ICPMS (HDC-ICPMS)*

HDC separates the compounds on the basis of their hydrodynamic diameter. The largest compounds elute first, followed by smaller ones. The separation occurs either in a column packed with inert, nonporous particles, or in a column packed with inert, porous particles, where the size of the pores is significantly smaller than the separated substances or in a capillary. The separation is based on the parabolic flow profile of the liquid in the column between the particles or in the capillary. In the middle of the profile are the fastest streamlines and the slowest are near the particles or the walls. Due to the fact that the larger compounds reach further into the flow profile they are transported faster, than smaller ones, which stay in the flow profile near the walls or particles, where the slower streamlines are. [43]

Tiede and co-workers spiked sewage sludge with 100 nm silver nanoparticles, mixed the solution for 6 hours and measured the supernatant with HDC-ICPMS. They observed two peaks with 59 nm and 3 nm average size, which weren't baseline separated. They used 6 gold nanoparticles standards to obtain an external calibration curve. They didn't use the gold nanoparticles as internal standards, whereas in a second experiment, they used gold nanoparticles as internal standard in a $Fe_2O_3$, $TiO_2$, $Al_2O_3$, $SiO_2$ nanoparticle containing mixture. They also didn't observe an ionic silver peak and also didn't spike the sewage sludge with just ionic silver. [44]

Lewis used a HDC-PCi-ICPMS system to determine the size of 42 nm PVP-AgNPs. He used gold nanoparticles to obtain an external calibration curve, but didn't use them as an internal standard. He used an HPLC system with an

autosampler with a dual injection mode and 2 pumps to do flow injections and on column injections of the same sample in the same run to calculate the column recovery. The column recovery was over 97 %. It is interesting to see that he didn't observe an ionic silver peak in his chromatograms, because he didn't purify the PVP-AgNPs prior to measurement. Instead they just diluted them with buffer solution and measured them. Further it is noteworthy that he used different flows for flow injections and on-column injections. [45]

### *1.9.10 Tangential flow ultrafiltration*

Tangential flow ultrafiltration uses a series of membrane modules with different pore sizes (1 nm up to 100 µm) to size select and concentrate a desired compound. [46]
Trefry and co-workers used a KrosFlo II Research System (Spectrum Laboratories, USA) to size select and concentrate uncoated AgNPs. They first filtered the samples through a 50 nm Midi Kros module and further with a 100 kD Midi Kros module. The original AgNP solution was polydisperse (90 % of particles between 1 – 25 nm). After ultrafiltration the solution consisted of concentrated, lowly aggregated AgNPs with a narrower size distribution (80 % of particles between 1 – 15 nm). [46]
This method is good to clean and concentrate a AgNP solution, but various offline detection methods, such as TEM, UV-Vis absorption and F-AAS, have to be applied to quantify and characterize the AgNPs.

## 1.10 HPLC

### *1.10.1 Size exclusion chromatography (SEC)*

In size-exclusion chromatography compounds are separated according their hydrodynamic diameter, in simpler terms, based on their size in solution. Large molecules elute first, followed by smaller ones. This is due to the exclusion of larger molecules from small pores, whereas small molecules can penetrate these small pores and remain longer in the column. The important difference to

other chromatography modes like RPC (reversed-phase chromatography) is that ideally the molecules don’t interact with the stationary phase. [47]

# 2 Experimental

## 2.1 Instruments

- 1260 Infinity HPLC system, Agilent, Germany including a 1260 HiP Degasser, a 1260 Bin Pump, a 1260 ALS, a 1290 Thermostat and a 1260 TCC
- Metal free HPLC system, Dionex, USA including a thermostatted column compartment (Dionex ICS 5000+ DC), an autosampler (Dionex AS) and a pump (Dionex ICS-3000)
- 7700x ICPMS, Agilent, Germany
- 7500ce ICPMS, Agilent, Germany
- Water purification system, Elix 3, Millipore, USA
- SubPUR subboiling system, MLS Milestone GmbH, Italy
- Sartorius balance, BL 210 S, Max 210 g, d = 0.1 mg, Germany
- 100 - 1000 µL pipette, Acura 825, Socorex, Switzerland
- 10 - 100 µL pipette, Acura 825, Socorex, Switzerland
- 0.5 - 5 mL pipette, Acura 835, Socorex, Switzerland

## 2.2 Materials

- 15 mL Tubes, polypropylene, P/N 188271, Greiner bio-one, Austria
- 50 mL Tubes, polypropylene, P/N 227261, Greiner bio-one, Austria
- 1.5 mL vials amber glass, P/N 548-0005, VWR International, Austria
- 1 mL crimp vials, polypropylene, P/N 8010-0159, CrossLab, Agilent, Germany
- 0.7 mL vials with snap ring, polypropylene, P/N 548-0895, VWR International, Austria
- Snap ring cap, red rubber/PTFE, P/N 548-3330, VWR International, Austria
- Crimp cap, red rubber/PTFE, P/N 548-3272, VWR International, Austria

## 2.3 Chemicals

- Nitric acid 69 % p.a., P/N X943.2, Roth, Germany
- Ultrapure water, 18.2 MΩ·cm, Millipore, USA
- Silver nitrate, P/N 7908.2, Roth, Germany
- Sodium borohydride, P/N 4051.2, Roth, Germany
- Polyvinylpyrrolidone, PVP, P/N PVP-40T, Sigma-Aldrich, USA
- Cetyltrimethylammoniumbromide, CTAB, P/N 2342, Merck, Germany
- Tri-sodium citrate dihydrate, P/N 106448, Merck, Germany
- Ammonium acetate, P/N 09690, Fluka, Switzerland,
- Sodium dodecylsulfate, SDS, P/N 2326.1, Roth, Germany
- Sodium thiosulfate, P/N 6516, Fluka, Switzerland

Nitric acid was further purified with the SubPUR subboiling system.

## 2.4 Standards

Peak Performance CRM, Single Element Standard, CPI International, USA

- Ag: concentration = 1000 ± 3 µg/mL in 2% $HNO_3$, P/N S4400-1000511
- Li: concentration = 1000 ± 3 µg/mL in 1% $HNO_3$, P/N S4400-1000291
- Rb: concentration = 1000 ± 3 µg/mL in 2% $HNO_3$, P/N S4400-1000451
- Sr: concentration = 1000 ± 3 µg/mL in 2% $HNO_3$, P/N S4400-1000531

ICP-Standard-Solution, single element, roti star, Roth, Germany

- Ba: concentration = 1000 mg/L ± 0.2 % in 1 % $HNO_3$, P/N 2400.1
- Ca: concentration = 10000 mg/L ± 0.2 % in 2 % $HNO_3$, P/N 2503.1
- Cs: concentration = 1000 mg/L ± 0.2 % in 2 % $HNO_3$, P/N 2406.1
- Mg: concentration = 10000 mg/L ± 0.2 % in 2 % $HNO_3$, P/N 2524.1

In-house standards

- Arsenate: concentration = 1000 mg As/L ($As^{V}$)
- Arsenite: concentration = 988.3 mg As /L ($As^{III}$)

## 2.5 Software

- MassHunter Workstation (G7201C Version C.01.01 Build 423.5)
- Microsoft Office Professional Plus 2010 (Version 14.0.7143.5000 32-Bit)
- Sigmaplot for Windows (Version 12.5 Build 12.5.0.38)

## 2.6 Synthesis of silver nanoparticles

*Citrate-AgNP (negatively charged surface coating).*

9 mg of $AgNO_3$ were dissolved in 50 mL of deionized water in a 50 mL polypropylene tube and transferred into a 100 mL round-bottom flask (solution A). The solution was heated to 80°C under vigorous stirring. Meanwhile, 68 mg tri-sodium citrate were dissolved in 7 mL deionized water in a 15 mL polypropylene tube (solution B). Solution B was added quickly in one portion, when solution A reached the temperature of 80°C. The temperature dropped to 75°C and then increased to a final temperature of 95°C. After one hour, when the reaction mixture turned greyish, the solution was immediately cooled down to room temperature by means of an ice bath to stop further reduction. The particles were transferred to 50 mL polypropylene tubes and stored at 4°C in the dark. The solution has a milky color and wasn't further purified. This procedure was modified from the work of Dement'eva and co-workers. [48]

*PVP-AgNP (nonionic surface coating).*

1 g of PVP was dissolved in 100 mL of deionized water in a 250 mL round-bottom flask. 5 mL of this solution were transferred into a 15 mL polypropylene tube. 40 mg of $AgNO_3$ were added to the remaining 95 mL of the PVP solution and dissolved completely under constant stirring (solution A). To the 5 mL portion of the PVP solution 16 mg of $NaBH_4$ were added and dissolved (solution B). After complete dissolution of the added solids, solution B was added dropwise (about 1 - 2 drops/sec.) to solution A. The reaction mixture was mixed vigorously at room temperature for 15 min. Afterwards the solution was then transferred to 50 mL polypropylene tubes and stored at 4°C in the dark.

The solution has a red color and wasn't further purified. This method is a modified procedure from the work of Malina and co-workers. [49]

*CTAB-AgNP (positively charged surface coating).*
17 mg $AgNO_3$ were dissolved in 50 mL of deionized water in a 250 mL round-bottom flask. Further 1.5 mL of a concentrated $NH_4OH$ solution were added and 5 minutes later 9 mg of CTAB were dissolved in the same solution (solution A). 16 mg $NaBH_4$ and 9 mg CTAB were dissolved completely in 50 mL deionized water in a 50 mL polypropylene tube (solution B). Solution B was added dropwise (about 1 – 2 drops/sec.) to solution A under vigorous stirring at ice-cold temperature for 4 h. Then the reaction mixture was heated for 1 hour (until the smell of ammonia is gone) with a mantle heater to drive out the remaining ammonia and to decompose the excess $NaBH_4$. Afterwards the mixture was cooled down to room temperature and transferred to 50 mL polypropylene tubes and stored at 4°C in the dark. The solution has a brownish-yellowish color and wasn't further purified. This is a modified procedure from the work of Sui and co-workers. [50]

## 2.7 Size determination of silver nanoparticles

For the size determination of the synthesized silver nanoparticles a dynamic light scattering (DLS) system was used. The equipment was composed of a goniometer and a diode laser (Coherent Verdi V5, λ = 532 nm, maximum output of 5 W) with single-mode fiber-detection optics (OZ from GMP, Switzerland). For data acquisition a photomultiplier, which was combined with pseudo cross correlation and an ALV5000/E correlator with fast expansion (ALV, Germany) was used. This allowed a minimum time interval of 12.5 ns for the correlation function. The ALV-5000/E software package was used to record and store the correlation functions. Correlation functions were collected 10 times, for 30 s each, and averaged. From these functions, an average diffusion coefficient D was obtained by using cumulant analysis. The software used for this was ORT for Windows (Preliminary Version 06.2008 by G. Fritz-Popovski). All experiments were carried out at 25°C and with a scattering angle of 90°. The

laser power for the experiments was between 10 and 200 mW, depending on the scattering power of the sample.

The various AgNP solutions were diluted with ultrapure water to a concentration of about 1 µg Ag/L before DLS measurement. The determined sizes of citrate, PVP and CTAB coated AgNPs can be found in Table 1. The measurement was done just once.

**Table 1:** Size of citrate, PVP and CTAB coated AgNPs determined with DLS (n = 1)

| | **citrate-AgNP** | **PVP-AgNP** | **CTAB-AgNP** |
|---|---|---|---|
| **Size [nm]** | ~ 16 | ~ 4 | ~ 80 |

## 2.8 Chromatography & Detection

The chromatography was performed with a 1260 Infinity HPLC system or a metal free HPLC system using either a SEC column or a RP-column. As detector a 7700x ICPMS was coupled to the HPLC system via a PEEK capillary. The instrument was tuned in no-gas mode before every measurement (see Table 2). A typical tuning solution consists of 1 µg/L Li, Y, Tl and Ce in 2 % $HNO_3$ (v/v).

**Table 2**: Typical ICPMS performance after tuning

| **Parameter** | **No-gas mode** |
|---|---|
| $^{7}Li$ [counts] | 4500 – 6000 |
| $^{89}Y$ [counts] | 9000 – 13000 |
| $^{205}Tl$ [counts] | 9000 – 13000 |
| Average RSD [%] | 2.5 – 3.2 |
| $^{140}Ce^{16}O^{+}/^{140}Ce^{+}$ [%] | 1.4 – 2.0 |
| $^{140}Ce^{2+}/^{140}Ce^{+}$ [%] | 1.2 – 1.9 |

The used columns and the used mobile phase are listed below.

**SEC column** Tosoh TSK-GEL SUPERSW3000, 300 mm x 4.6 mm ID, particle size 4 µm, pore size 250 Å, silica based with functional group: diol

**RP column** Altmann Analytik, 250 mm x 4.6 mm ID, particle size 7 µm, pore size 1000 Å, stationary phase: NUCLEOSIL C18

**Mobile phase/HPLC buffer**: 10 mmol/L ammonium acetate (771 mg/L), 10 mmol/L sodium dodecyl sulfate (SDS, 2884 mg/L), 1 mmol/L sodium thiosulfate pentahydrate (248 mg/L), pH = 6.6.

# 3 Results and discussion

The various AgNP solutions weren't further purified after synthesis. The total silver concentrations of the silver nanoparticle solutions were determined with ICPMS after dilution with ultrapure water (Table 3).

**Table 3**: Concentration of various synthesized silver nanoparticles

| | **Citrate-AgNP** | **PVP-AgNP** | **CTAB-AgNP** |
|---|---|---|---|
| **Total Ag concentration [mg/L]** | 121 ± 7 | 227 ± 4 | 103 ± 8 |

## 3.1 First measurements of AgNPs

The AgNP solutions were diluted with ultrapure water in HPLC glass vials. The samples were measured without the column (flow injection) and with the installed column (Kinetex: reversed phase C18, 5 µm, 100 Å, 250 x 4.6 mm) to calculate the column recovery. The measurement of the three AgNP types and an ionic silver solution resulted in erratic measurement results. For example the determined column recovery for cit-AgNPs was over 500 %. Because of these results, although it was just a single measurement, the concentration of the solutions was measured again with ICPMS only. Therefore the samples were diluted with ultrapure water once in glass vials and once in PP vials.

**Table 4**: Nominal silver concentration and measured silver concentration in different storage containers

| | **Nominal value [µg Ag/L]** | **glass vial storage [µg Ag/L]** | **PP vial storage [µg Ag/L]** |
|---|---|---|---|
| **Citrate-AgNP** | 12 | ~ 0.4 | ~ 7.2 |
| **PVP-AgNP** | 11 | ~ 0.5 | ~ 5.7 |
| **CTAB-AgNP** | 10 | ~ 0.7 | ~ 2.0 |
| **Ionic silver** | 5 | ~ 1.4 | ~ 6.1 |

Because of the results shown in (Table 4) further stability experiments were performed.

Possible reasons causing these problems are: the AgNP solutions were diluted with water and not in the HPLC buffer; the AgNPs or free ionic silver may be adsorbed by the glass walls of the HPLC vials; the solutions weren't acidified

prior to the measurements with the ICPMS which could result in adsorption in the tubings of the sample introduction system.

## 3.2 Stability of the measurement solutions

The idea of the stability experiment was to simulate a whole day of measurement. Therefore, the different silver nanoparticles were stored under different conditions and concentrations. The storage vials consisted either of polypropylene (PP) or glass. The storage solution was either HPLC-buffer or ultrapure water.

### *3.2.1 Citrate-AgNP storage comparison*

For this experiment the citrate-AgNPs were diluted with the mobile phase and stored at 3 different concentrations [10, 100, 1000 µg Ag/L]. For the measurement with the ICPMS the higher concentrated samples were further diluted to a final concentration of ~10 µg Ag/L. The samples were measured straight after preparation (hour 0), 4 hours after preparation (hour 4), 8 hours after preparation (hour 8) and 24 hours after preparation (hour 24). The results of these measurements can be seen in Figure 2.

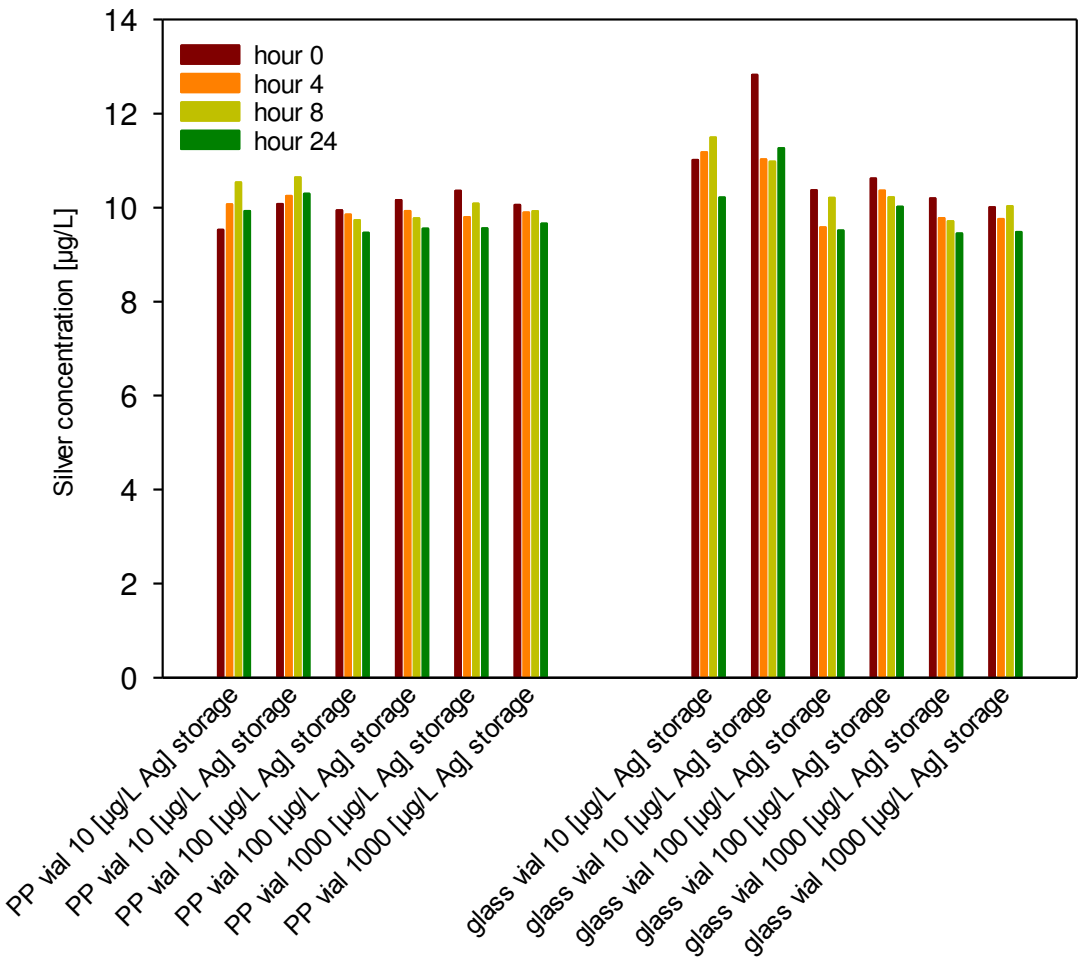


**Figure 2**: Citrate-AgNPs diluted with mobile phase stored in glass or PP vials

In a further experiment the citrate-AgNPs were diluted with ultrapure water and stored at 3 different concentrations [10, 100, 1000 µg Ag/L]. For the measurements with the ICPMS the higher concentrated samples were further diluted to a final concentration of 10 µg Ag/L. The samples were measured straight after preparation (hour 0), 4 hours after preparation (hour 4), 8 hours after preparation (hour 8) and 24 hours after preparation (hour 24). The results of these measurements can be seen in Figure 3.

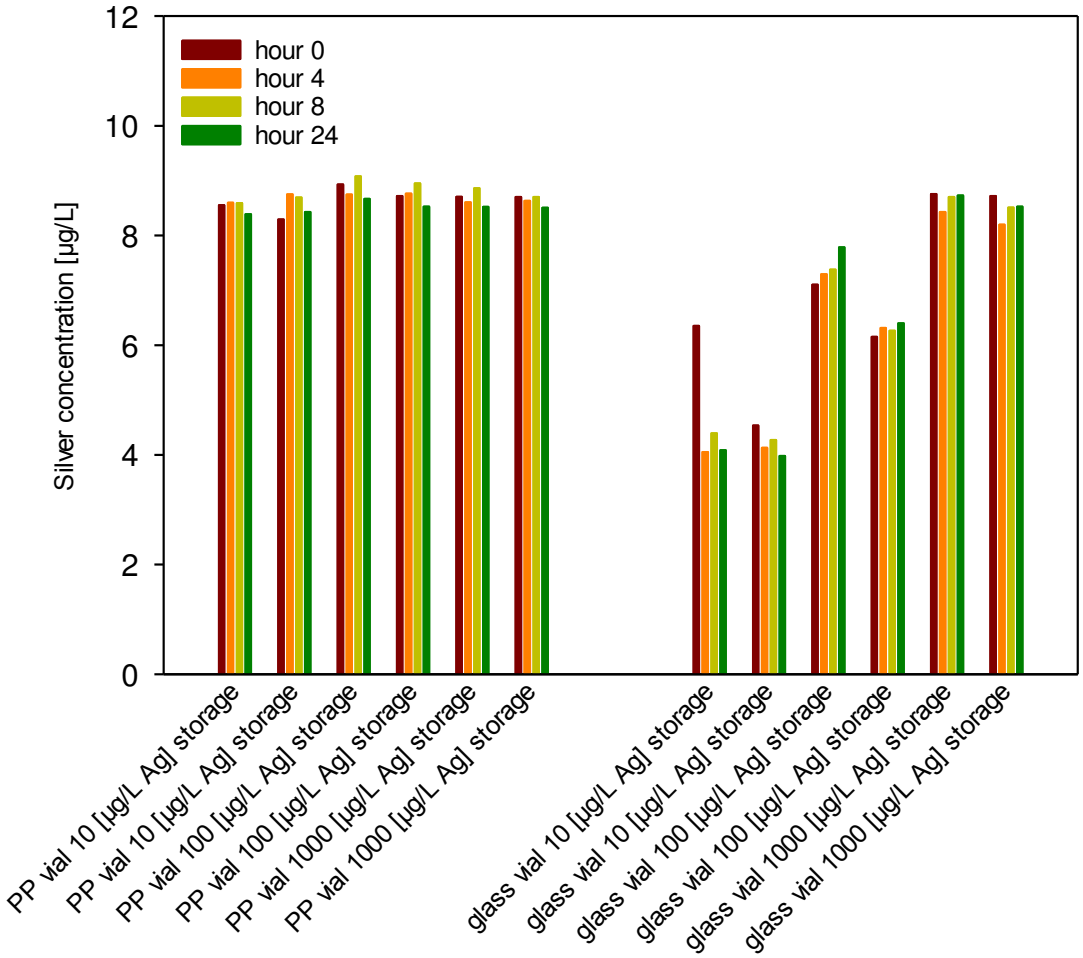


**Figure 3**: Citrate-AgNP diluted with ultrapure water stored in glass or PP vials

To confirm the trend shown in Figure 3, the storage experiment, regarding citrate-AgNP stored in glass vials and diluted with ultrapure water, was repeated with more different concentrations. In Figure 4 the results of this experiment are shown.

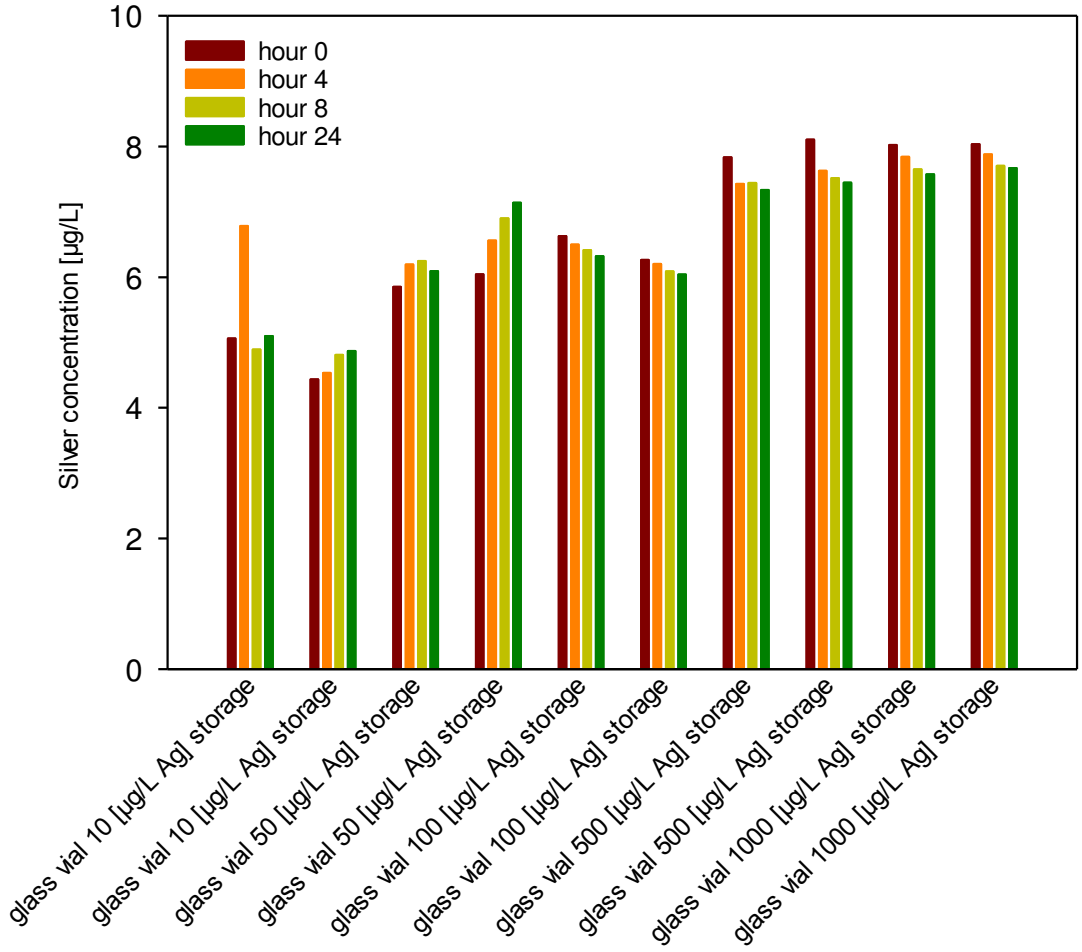


**Figure 4**: Citrate-AgNP diluted with ultrapure water stored in glass vials

### *3.2.2 PVP-AgNP storage comparison*

For this experiment the PVP-AgNPs were diluted with the mobile phase and stored at 3 different concentrations [12, 120, 1200 µg Ag/L]. For the measurement with the ICPMS the higher concentrated samples were further diluted to a final concentration of 12 µg Ag/L. The samples were measured straight after preparation (hour 0), 4 hours after preparation (hour 4), 8 hours after preparation (hour 8) and 24 hours after preparation (hour 24). The results of these measurements can be seen in Figure 5.

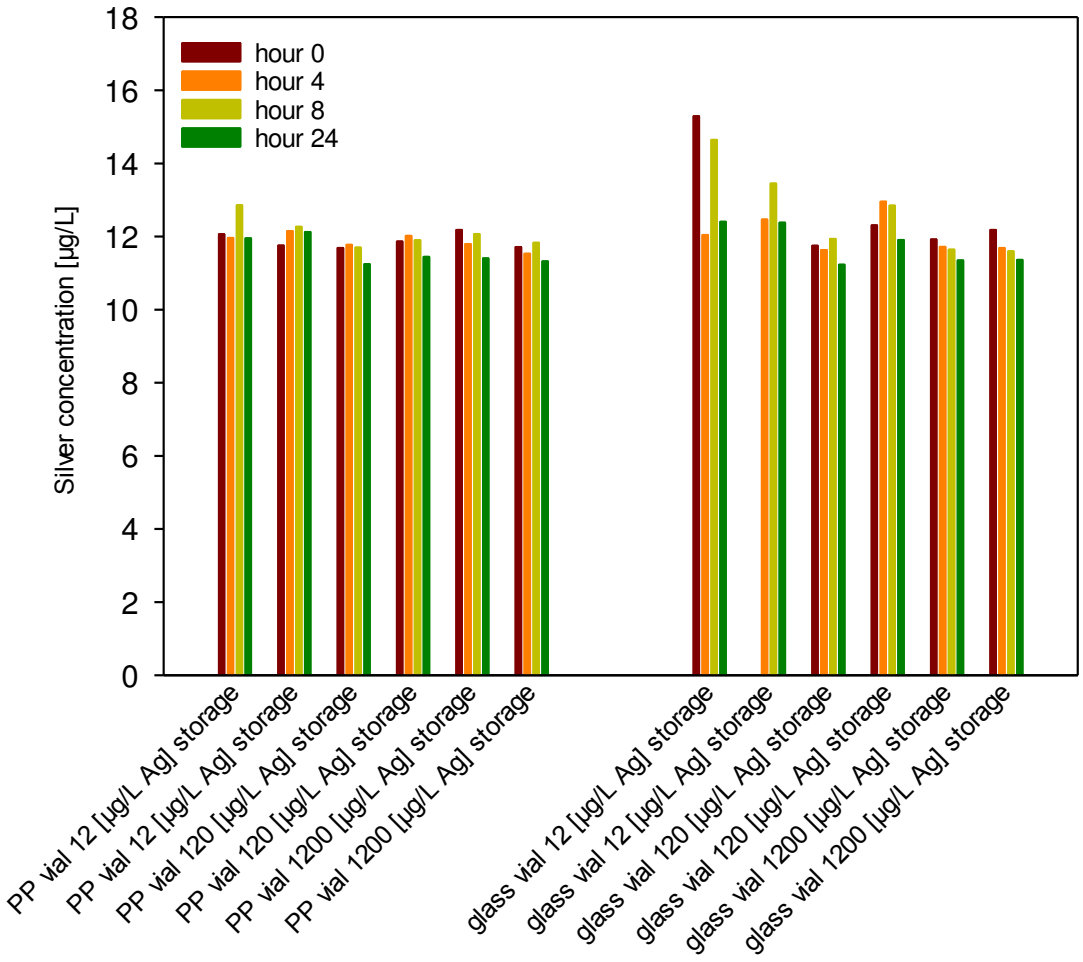


**Figure 5**: PVP-AgNPs diluted with mobile phase stored in glass or PP vials

In a further experiment the PVP-AgNPs were diluted with ultrapure water and stored at 3 different concentrations [12, 120, 1200 µg Ag/L]. For the measurement with the ICPMS the higher concentrated samples were further diluted to a final concentration of 12 µg Ag/L. The samples were measured straight after preparation (hour 0), 4 hours after preparation (hour 4), 8 hours after preparation (hour 8) and 24 hours after preparation (hour 24). The results of this measurement can be seen in Figure 6.

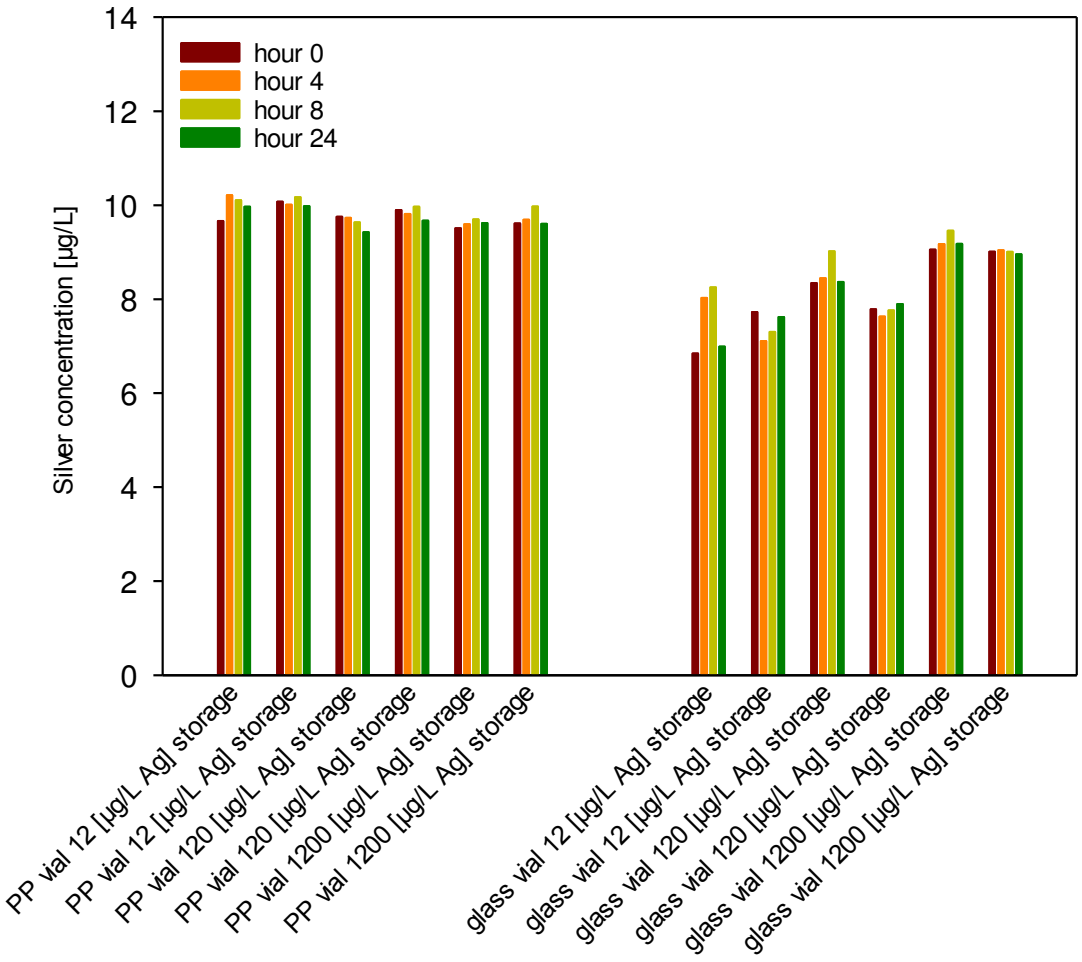


**Figure 6**: PVP-AgNPs diluted with ultrapure water stored in glass or PP vials

### *3.2.3 CTAB-AgNP storage comparison*

For this experiment the CTAB-AgNPs were diluted with the mobile phase and stored at 3 different concentrations [20, 200, 2000 µg Ag/L]. For the measurement with the ICPMS the higher concentrated samples were further diluted to a final concentration of 20 µg Ag/L. The samples were measured straight after preparation (hour 0), 4 hours after preparation (hour 4), 8 hours after preparation (hour 8) and 24 hours after preparation (hour 24). The results of this measurement can be seen in Figure 7.

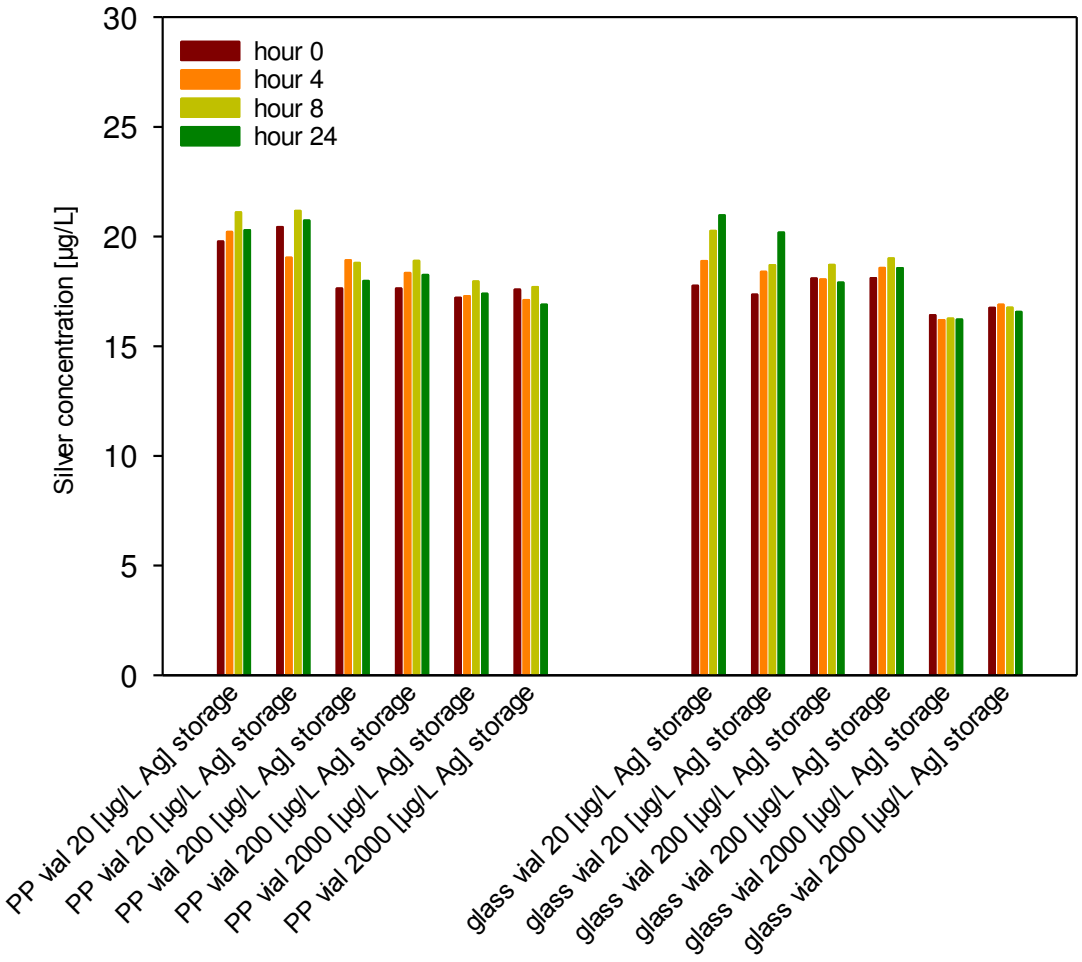


**Figure 7**: CTAB-AgNPs diluted with mobile phase stored in glass or PP vials

In a further experiment the CTAB-AgNPs were diluted with the ultrapure water and stored at 3 different concentrations [20, 200, 2000 µg Ag/L]. For the measurement with the ICPMS the higher concentrated samples were further diluted to a final concentration of 20 µg Ag/L. The samples were measured straight after preparation (hour 0), 4 hours after preparation (hour 4), 8 hours after preparation (hour 8) and 24 hours after preparation (hour 24). The results of this measurement can be seen in Figure 8.

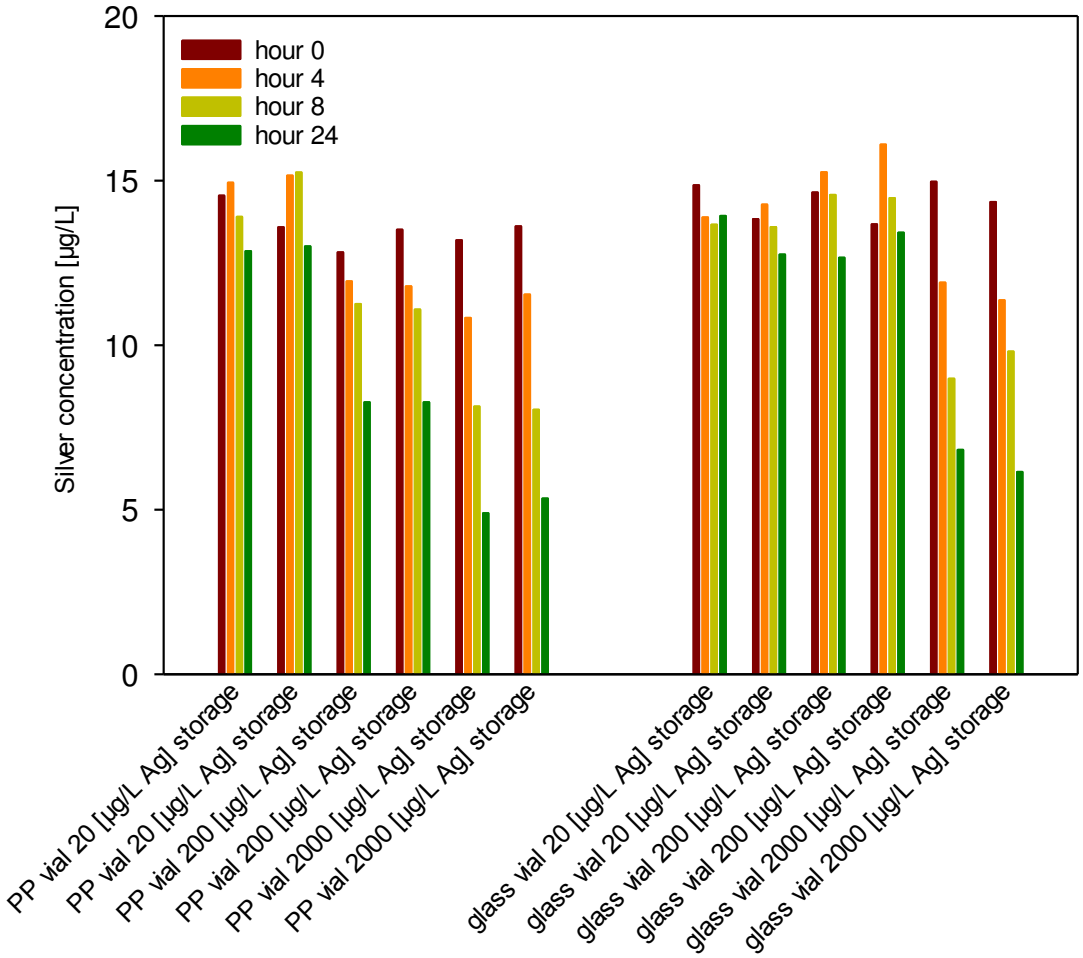


**Figure 8**: CTAB-AgNPs diluted with ultrapure water stored in glass or PP vials

To validate the trend shown in Figure 8, the experiment regarding CTAB-AgNPs diluted with ultrapure water was done once more with more different concentrations. Because of the more pronounced decrease of the Ag concentration over 24 hours in PP as container material, the experiment was repeated with this storage material. In Figure 9 the results can be seen.

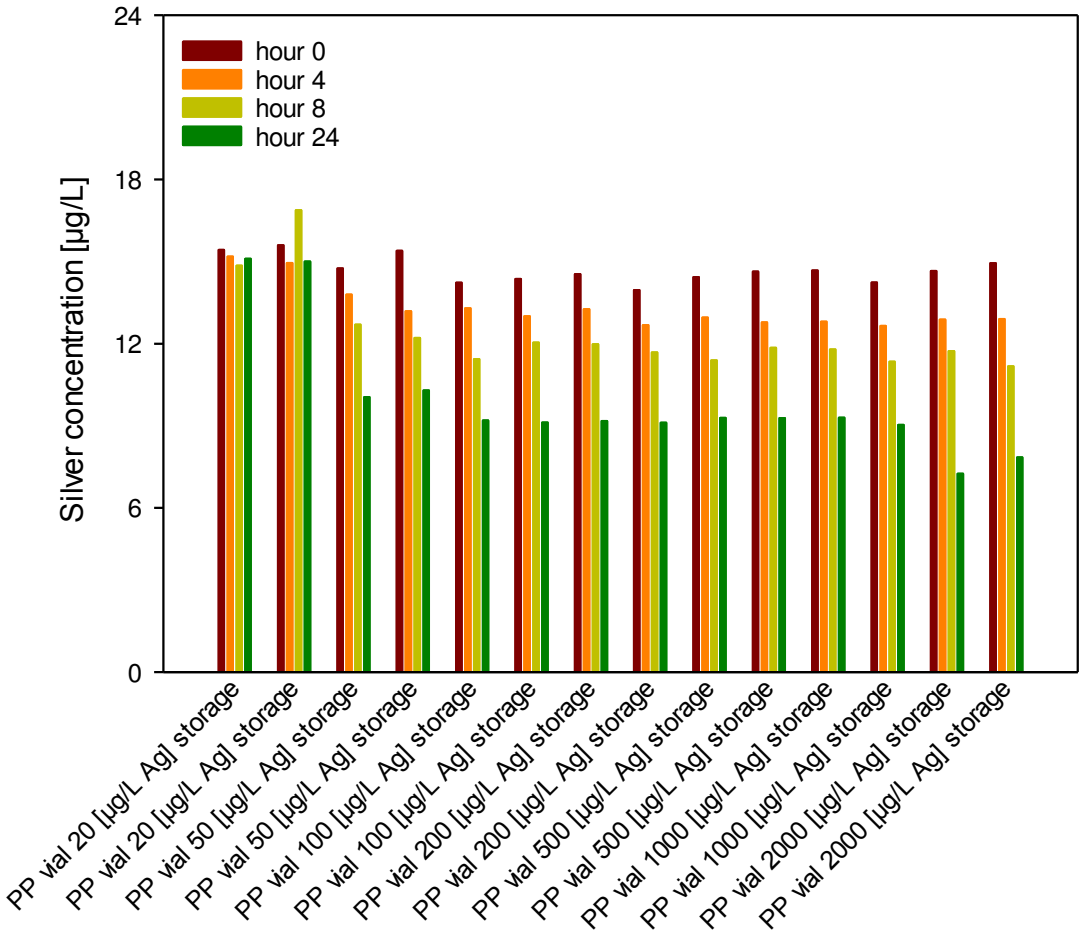


**Figure 9**: CTAB-AgNPs diluted with ultrapure water stored in PP vials

Possible reasons for the different stability of the silver concentration in the various measurement solutions are discussed below.

Silicate glass surfaces have a negative surface charge density when they are immersed in water. This is because of the dissociation of terminal silanol groups, like it is shown in following reaction equation: $SiOH \leftrightarrow SiO^- + H^+$. The degree of dissociation depends on the equilibrium between ions at the glass surface and ions in the solution [51].

This might be an explanation for the results shown in Figures 4 & 6 respectively for cit-AgNP and PVP-AgNP solutions. The solutions are diluted with ultrapure water, in which no free ions should be present. Free silver ions ($Ag^+$), which might be present in the nanoparticle solutions due incomplete reduction at the nanoparticle formation process or are present in ionic form again due to oxidation of the nanoparticles, may bind to the dissociated silanol groups, what

results in a decrease of the detectable silver concentration. In HPLC-buffer as storage medium (Figures 2 & 5) a great excess of free cations, such as sodium ions ($Na^+$) or ammonium ions ($NH_4^+$) are present and occupy the negatively charged silanol groups, whereby binding possibilities of the silver ions ($Ag^+$) to the silanol groups are reduced. The surface of polypropylene vials can be seen as unpolar and because of that an adsorption of $Ag^+$ ions can be excluded.

In the case of CTAB-AgNPs it is even more complicated. As it can be seen in Figure 8, where ultrapure water as a storage medium was used, the measured silver concentration is about one third lower than with mobile phase as a storage medium (Figure 7), although it should contain the same amount of silver. Further there is also a decrease in the detectable silver concentration over 24 hours (Figures 8 & 9), when ultrapure water as a storage medium is used, independent from the vial material. It is interesting to see, that the higher the silver concentration is, the larger the decrease of the measured concentration is. What's even more fascinating is the fact, that there is nearly no decrease over 24 hours for the 20 µg/L concentration. It is also shown that the silver concentration decrease happens in both storage vial materials and is even more pronounced for PP as vial material. Because of that, adsorption of free $Ag^+$ ions just plays a minor role.

Chakraborty and co-workers examined the $CTA^+$-bilayer of CTAB-AgBr nanoparticles. Although the synthesis is quite different (Chakraborty [52] first forms AgBr colloids, which are then stabilized with $CTA^+$, whereas Sui [50] first forms diaminesilver, which is further reduced to silver particles and then stabilized with $CTA^+$) the $CTA^+$-bilayer should be the same for both particle types. By measuring the ζ potential Chakraborty and co-workers found out, that first a monolayer with randomly orientated $CTA^+$ ions forms around the particle, which is reflected in a lower ζ potential value. After $CTA^+$ bilayer formation the ζ potential was higher and remained constant. With "DSC-TGA analysis" they ensure the $CTA^+$ bilayer structure around the particle. Further they point out, that the $CTA^+$ has 2 different orientations. They suggest a first layer closer to the particle with the N-containing headgroup attached to the particle and a second layer, where the N-containing headgroup is protruding in the ambient solvent. With NMR Spectroscopic studies they proved that the $CTA^+$ is attached to the silver particle with the nitrogen containing headgroup [52].

Liu and co-workers used CTAB to aggregate silica nanoparticles. They measure a negative ζ potential at very low $CTA^+$ concentrations and a positive ζ potential value at very high $CTA^+$ concentrations. They further observe no aggregation of the silica nanoparticles at very high and very low $CTA^+$ concentrations but at mid-level $CTA^+$ concentrations they notice aggregation of the particles [53].
In the undiluted CTAB-AgNP synthesis solution a very high $CTA^+$ concentration is present. Therefore a $CTA^+$ bilayer is around the AgNPs and aggregation of the AgNPs is avoided. Due to dilution of the synthesis solution for measurment, the $CTA^+$ concentration is reduced. Therefore, in the diluted solutions a part of the outer layer might be dismantled, an unstructured $CTA^+$ layer remains and aggregation of the particles might be possible. In the 20 µg/L storage solution the ζ potential of the particles might already be negative enough to avoid aggregation. The agglomerated AgNPs or due to oxidation of the AgNPs released $Ag^+$ ions might stick to the sample introduction tubings. Another reason could be the adsorption of the CTAB-AgNPs on the vial surfaces and/or the sample introduction tubings, because of the amphiphilic characteristic of CTAB. Because of that, the amount of detectable silver is independent from the vial material (Figures 7, 8 & 9).
As the results show, it is crucial for analysis how the AgNP solutions are prepared for the analysis. The container material, the dilution media and the storage time should be mentioned in the experimental part of papers to comprehend any results. Whether these effects shown above are from the AgNPs themselves or from ionic silver or from both silver species, requires further investigation. As a consequence of these experiments only PP HPLC vials and mobile phase as dilution medium are used for further investigation of AgNP solutions because at least the detectable silver concentration is stable for 24 hours.

### 3.3 Retention behavior of various substances on a TSK-GEL SUPERSW3000 column

The TSK-Gel SUPERSW3000 consists of spherical silica particles with very high internal pore volumes. The particles are functionalized with polar diol groups. To get a better understanding of the retention behavior of the column, elements or compounds with following characteristics were chosen: single positively charged ($Li^+$, $Rb^+$, $Cs^+$, $Ag^+$), double positively charged ($Mg^{2+}$, $Ca^{2+}$, $Sr^{2+}$, $Ba^{2+}$), uncharged (arsenite) and negatively charged (arsenate, cit-AgNP). The experiment was done twice. 10 µL of a mixture containing 100 µg/L (Li, Rb, Cs, Mg, Sr, Ba, Ag, $As^{III}$, $As^{V}$), 1 mg/L (Ca) and ~ 130 µg/L (cit-AgNP) were injected twice consecutively. The reproducibility of this measurement was quite good, as it can be seen in Figures 10 & 11.

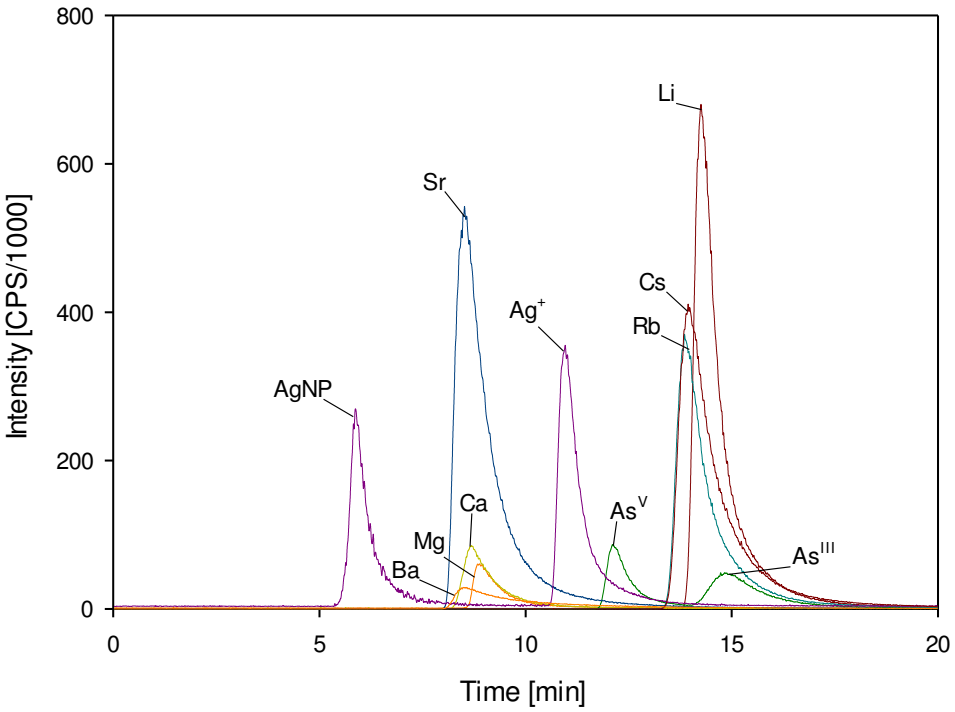


**Figure 10**: Chromatogram of a mixture containing 100 µg/L (Li, Rb, Cs, Mg, Sr, Ba, Ag, $As^{III}$, $As^{V}$), 1 mg/L (Ca) and ~ 130 µg/L (cit-AgNP) separated with a TSK-GEL SUPERSW3000 column

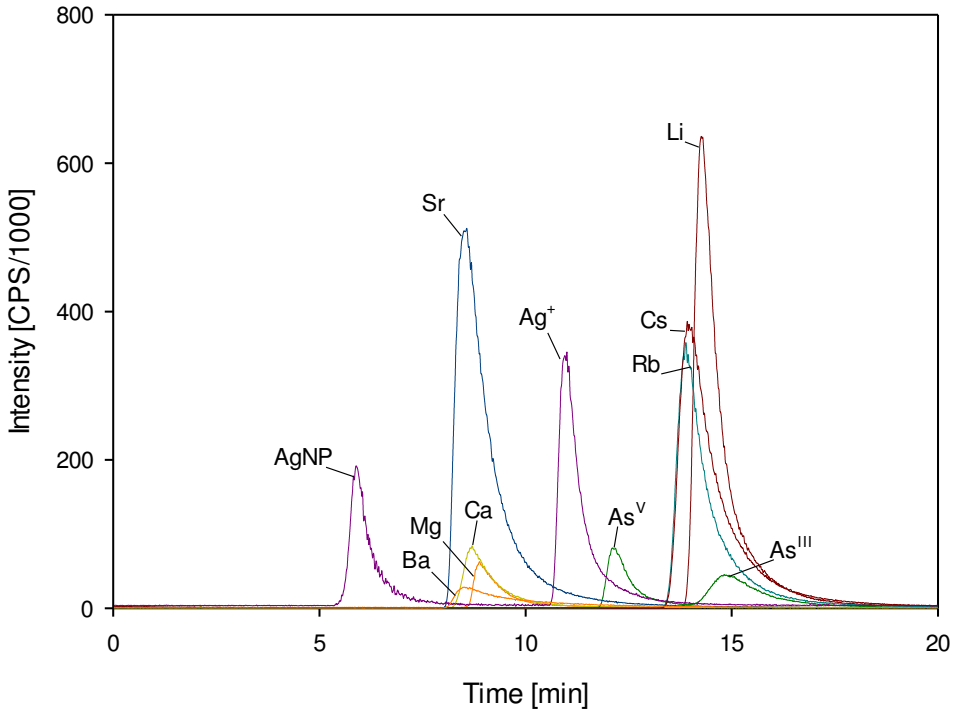


**Figure 11**: Chromatogram of a mixture containing 100 µg/L (Li, Rb, Cs, Mg, Sr, Ba, Ag, $As^{III}$, $As^{V}$), 1 mg/L (Ca) and ~ 130 µg/L (cit-AgNP) separated with a TSK-GEL SUPERSW3000 column

The compounds are listed according to their elution order respectively their retention time and their column recovery can be found in Table 5. The column recovery was calculated by comparing the peak area from a flow injection to the area obtained after TSK-GEL SUPERSW 3000 column separation.

**Table 5:** Retention time and column recovery of Li, Rb, Cs, Mg, Sr, Ba, Ag, $As^{III}$, $As^{V}$, Ca and cit-AgNPs on a TSK-GEL SUPERSW 3000 column; the hydrated radius of $As^{III}$ & $As^{V}$ was calculated with the Stokes-Einstein-equation and the diffusion coefficient given by Tanaka et al. [54], n. d. - not determined, n. f. - not found

| Element | RT [min] | Column recovery [%] | Ionic radius [nm][55] | Hydrated radius [nm] |
|---|---|---|---|---|
| **cit-AgNP** | 5.9 | n. d. | n. f. | 16 |
| **Sr** | 8.5 | 80 | 0.113 | 0.412[55] |
| **Ba** | 8.6 | 96 | 0.135 | 0.404[55] |
| **Ca** | 8.7 | 83 | 0.099 | 0.412[55] |
| **Mg** | 8.8 | 74 | 0.065 | 0.428[55] |
| **Ag** | 11.0 | n. d. | 0.126 | 0.341[55] |
| **$As^{V}$** | 12.1 | n. d. | n. f. | 0.302[54] |
| **Rb** | 13.9 | 59 | 0.148 | 0.329[55] |
| **Cs** | 14.0 | 51 | 0.169 | 0.329[55] |
| **Li** | 14.3 | 88 | 0.060 | 0.382[55] |
| **$As^{III}$** | 14.8 | n. d. | n. f. | 0.211[54] |

The results were quite surprising, because the earth alkali metals all elute around 8.6 minutes and the alkali metals elute around 14 minutes. This elution order can't be because of their ionic radius, because their ionic radius is increasing within their group. If the ionic radius determines the elution order, then for example Li should elute at the same time as Mg, which is not the case. But their hydrated radius seems to be a reason for the observed elution order of the alkali and earth alkali metals. The earth alkali metals all have a hydrated radius above 400 nm and elute before the alkali metals which all have a hydrated radius lower than 400 nm. Further it is prominent that the two negatively charged compounds elute at completely different times: cit-AgNPs after 5.9 minutes and $As^{V}$ after 12.1 minutes, which might be because of their different sizes (16 nm & 0.302 nm). The neutral $As^{III}$ elutes last after 14.8 minutes. The hydrated radius of the monovalent $As^{V}$ is 0.302 nm and for the neutral $As^{III}$ is 0.211 nm. Both hydrodynamic radii are lower than the radii of the alkali metals, but $As^{V}$ is eluting before the alkali metals and $As^{III}$ around the same time.

As all the hydrated radii are determined in pure water and the mobile phase consists of various ionic and complexing substances, the hydrodynamic radius of the various ions or molecules might be different as the one determined in water. Further the hydrated radius of ionic silver should be irrelevant, because there should be a complexation of the silver ion with thiosulfate and because of that, the hydrated radius of the complex should be known to interpret the elution time. Unfortunately, no hydrodynamic radius for the complex could be found. Further the complex might have a different retention mechanism than the ionic silver alone, because it might be interacting with the stationary phase. All in all it's difficult to say for all the studied ions, whether the retention mechanism is solely based on size exclusion or if it is due to the interaction of the various analytes with the stationary phase. For example there is a slight probability that earth alkali metals might be complexed by acetate according to Bjerrum [56]. This complex might have a bigger hydrodynamic diameter than the earth alkali metals alone. Also the interaction of the complexed alkali metals with the stationary phase might be different than for the single metal ions. Further it is possible, that they interact with the SDS modified stationary phase on their own

or maybe as an acetate complex. The possible modification of the stationary phase is mentioned in the FAQ section of the Technical Support of TOSOH, because they mention, that the column might be irreversible modified when additives like SDS are used in the mobile phase [57].
In the case that the retention mechanism for cit-AgNPs is solely based on size exclusion, the mechanism might looks like this: they may elute either with the interstitial volume ($V_0$), when they are too big to penetrate the pores or somewhere between $V_0$ and the dead volume ($V_m$). $V_m$ is $V_0$ plus $V_i$, which is the volume of the pore system. [47]

Experimental setup: HPLC 1260, ICPMS 7700x, TSK-GEL SUPERSW3000 column, flow rate 0.38 [mL/min].

## 3.4 Various reproducibility problems with the separation of ionic silver from citrate coated silver nanoparticles with a TSK-GEL SUPERSW3000 and a C18 column

In various chromatographic measurements of different coated AgNPs, either no AgNPs or just a small fraction of the AgNPs eluted from the column, depending on their coating. At these measurements the column recovery of the cit-AgNPs was quite bad, nevertheless the highest from all the analyzed AgNPs. Out of this, the goal of further experiments was to figure out which parameters are responsible for a good column recovery. Therefore, the focus was shifted towards the cit-AgNPs. In the course of these experiments it was observed, that when the same cit-AgNP solution was injected several times, that at the first and second injection there is nearly no AgNP signal. After several more injections the AgNP signal increases whereas the ionic silver signal stays nearly the same. Hereafter, a rough sequence of the performed measurements, their results and the respective conclusion out of them are listed.

### *3.4.1 Flooded spray chamber*

In a failed experiment, where the spray chamber was flooded, two cit-AgNP injections were made shortly before the ICPMS shutdown. The AgNP signal

was quite dominant already in the chromatograms of the first two injections (see Figure 12).

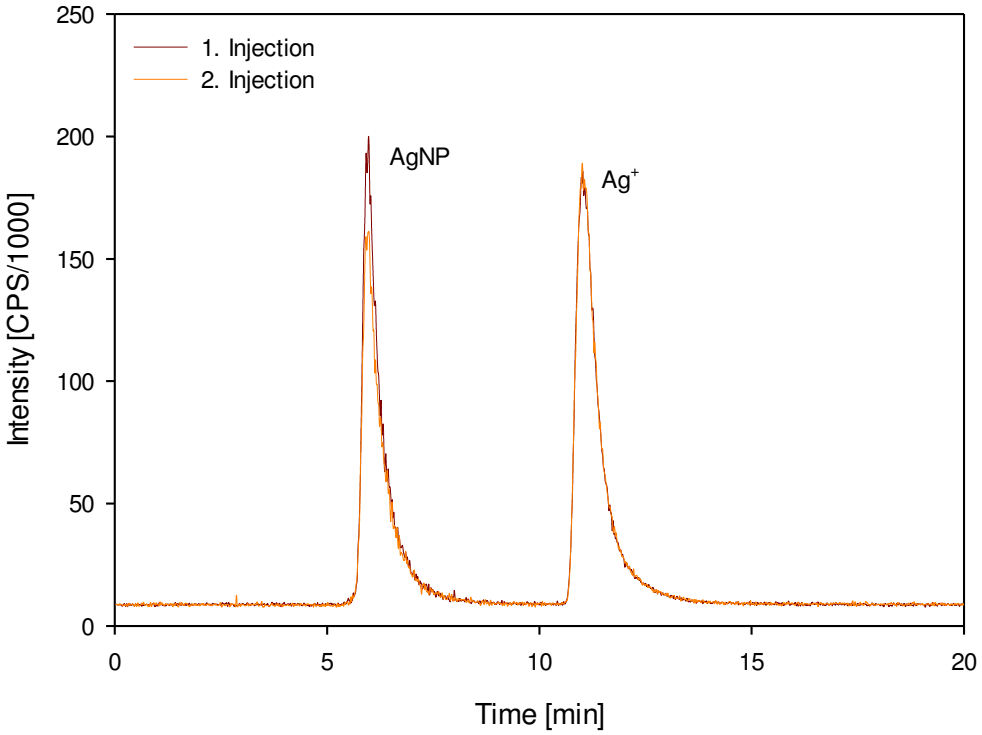


**Figure 12**: Chromatogram of a cit-AgNP solution shortly before a flooded spray chamber, containing cit-AgNPs and ionic silver, total silver amount in solution: 130 µg/L Ag.

The reason why this observation was quite important is, that in prior experiments the AgNP signal wasn't really visible. Because of that it was assumed, that maybe the sample transport in the spray chamber is insufficient and only because of the reduced volume in the spray chamber the AgNPs were able to reach the plasma this time and could be detected.

Experimental setup: HPLC 1260, ICPMS 7700x, TSK-GEL SUPERSW3000 column, flow rate 0.38 [mL/min].

### *3.4.2 Sample transportation experiment*

To proof the prior assumption that the sample transport to the plasma might be insufficient, an experiment with different carrier gas flows was conducted to simulate different sample transport conditions from the spray chamber to the plasma (see Figures 13 & 14).

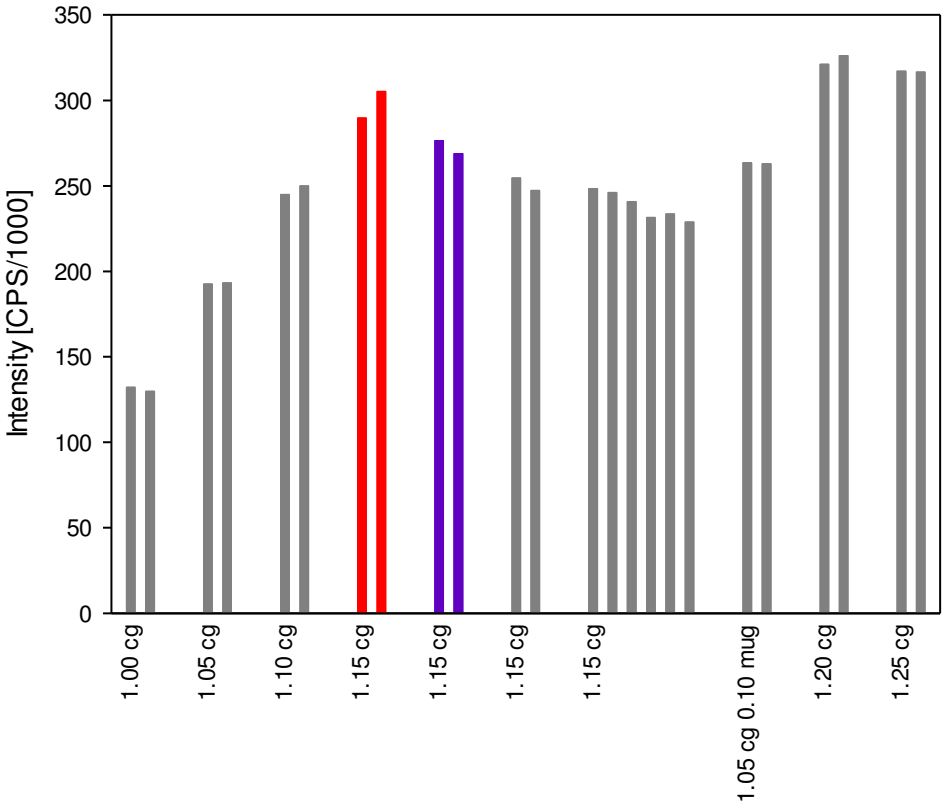


**Figure 13**: Diagram of the influence of various carrier gas (cg) flows [L/min] and make up gas (mug) flows [L/min] on the measured intensity of the ionic silver content of a cit-AgNP solution, total silver amount of the cit-AgNP solution: 130 µg/L Ag.

As it can be seen in Figure 13, the reproducibility of the ionic silver (red and purple bars have nearly the same height) is quite OK. The trend is, that the higher the carrier gas flow is, the higher the detectable silver concentration is. The slight difference between the results of a double determination at the same carrier gas flow rate is because of the slight variation of the chromatography. Also the difference of the signal intensity at 1.15 L/min carrier gas flow is due the variation in chromatographic behaviour of the ionic silver and not because of the measurement reproducibility of the ICPMS.

The increase of the signal intensity with higher carrier gas flows was also observed by Wang and co-workers. They observed that the intensity reaches a maximum at a certain carrier gas flow. But the intensity is dependent on many parameters of the instrument, like for example the applied rf-power. [58].

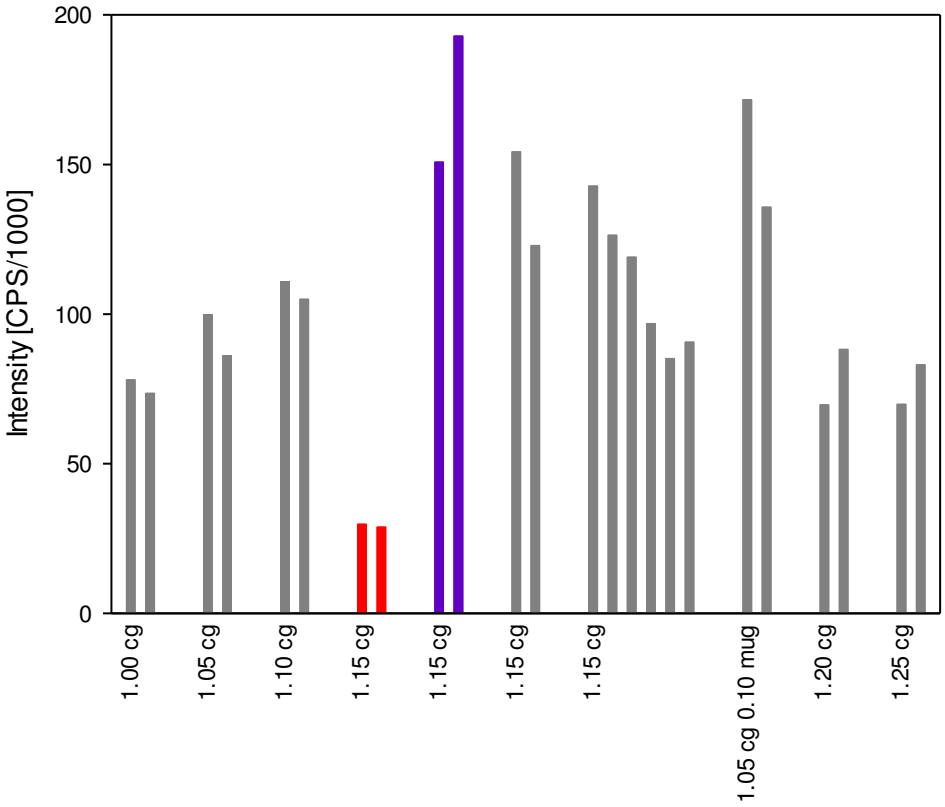


**Figure 14**: Diagram of the influence of various carrier gas (cg) flows [L/min] and make up gas (mug) flows [L/min] on the measured intensity of the AgNP content of a cit-AgNP solution, total silver amount of the cit-AgNP solution: 130 µg/L Ag.

Opposite are the results for the AgNPs (Figure 14). It absolutely didn't follow the presumption that the higher the carrier gas flow is, the higher the signal for the AgNPs is. Also the reproducibility of the AgNP signal is really bad at the same carrier gas flow rate (red and purple bars don't have the same height). This experiment was actually done twice with the same results. With a closer look on the measurement sequence (Figure 15) a time relation caught the eye.

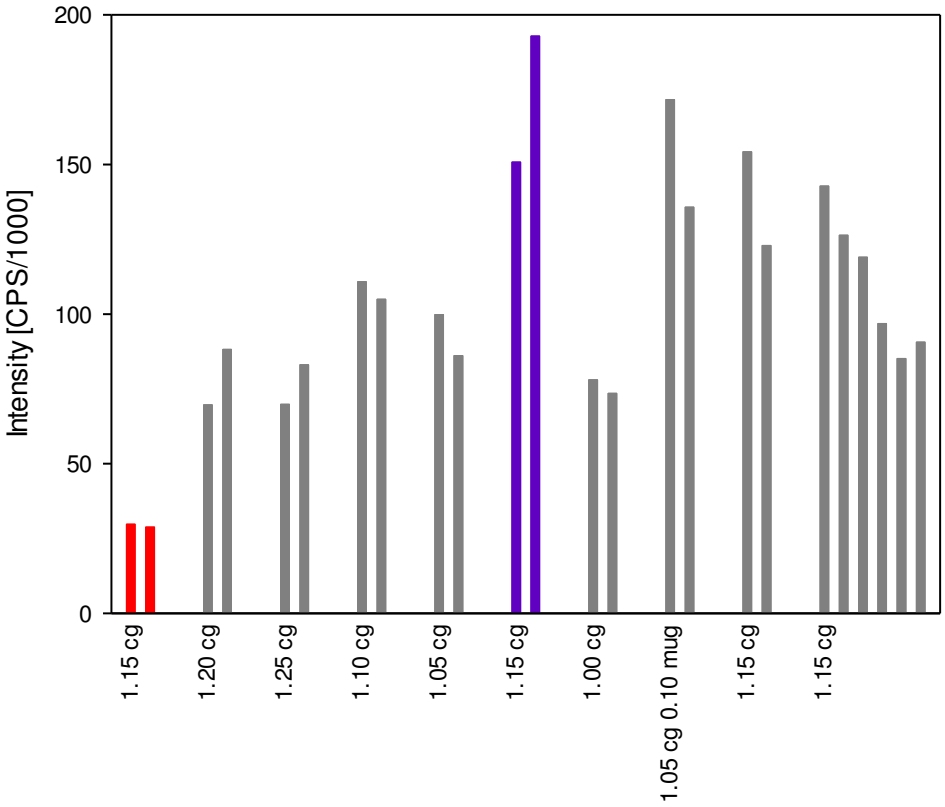


**Figure 15**: Diagram of the influence of various carrier gas (cg) flows [L/min] and make up gas (mug) flows [L/min] on the measured intensity of the AgNP content of a AgNP solution with consideration of the sequence order, total silver amount of the cit-AgNP solution: 130 µg/L Ag.

If the first assumption with the insufficient sample transport would be right, then the two peak areas (red and purple bars in Figure 15) should be the same for a carrier gas flow of 1.15 [L/min]. As it clearly can be seen, this is not the case. Because of this, another reason came in mind. Maybe the spray chamber needs to be conditioned with mobile phase for a certain amount of time, before a reproducible AgNP detection is possible. This idea is supported by the time the various chromatograms (Figure 16) were taken. The measurements of the same cit-AgNP solution with the same carrier gas flow of 1.15 [L/min] were done at time point 0, 1 hour later and another 2.5 hours later.

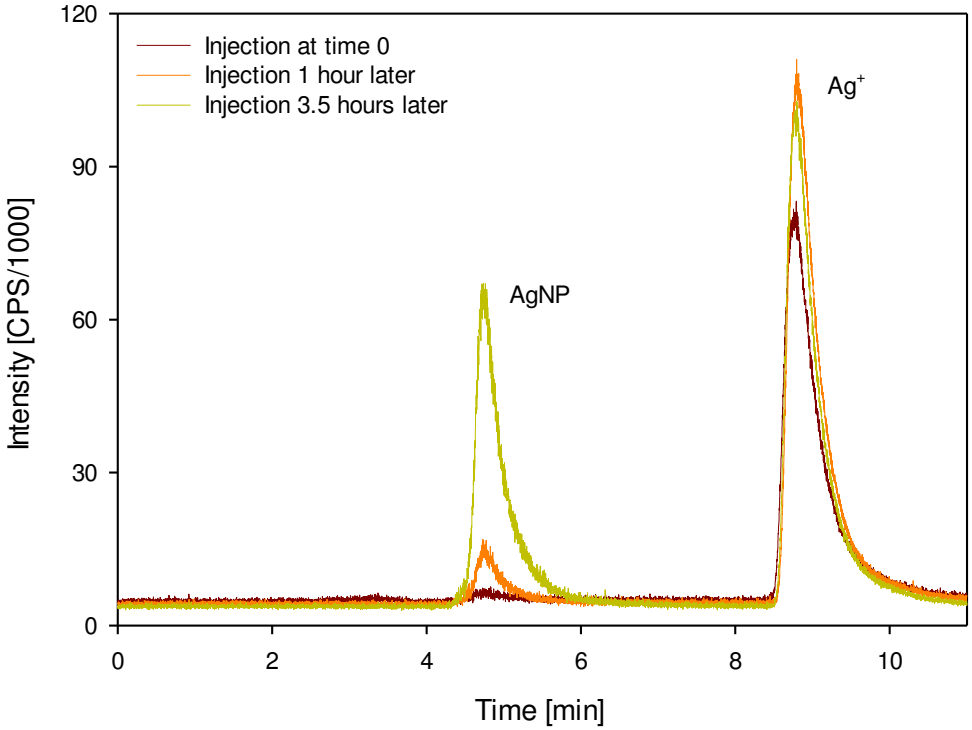


**Figure 16**: Change of the measured AgNP and ionic silver content over the time of 3.5 hours in the same AgNP solution, total silver amount of cit-AgNP solution: 130 µg/L Ag.

It is also important to mention, that the focus was on the insufficient AgNP transport, because the ionic silver signal was quite reproducible all the time, independent of the injection time. The slightly increased $Ag^+$ signal might be because of the destruction of the AgNPs over time in the mobile phase.

Experimental setup: HPLC 1260, ICPMS 7700x, TSK-GEL SUPERSW3000 column, flow rate 0.38 mL/min.

### *3.4.3 Conditioning of the spray chamber with mobile phase*

To proof the suspicion, that the spray chamber, the connection piece to the torch or the torch have to be conditioned with mobile phase to improve the AgNP transport, another experiment was conducted. After coupling the HPLC with the ICPMS another 3 h passed before the first cit-AgNP sample was injected (Figure 17).

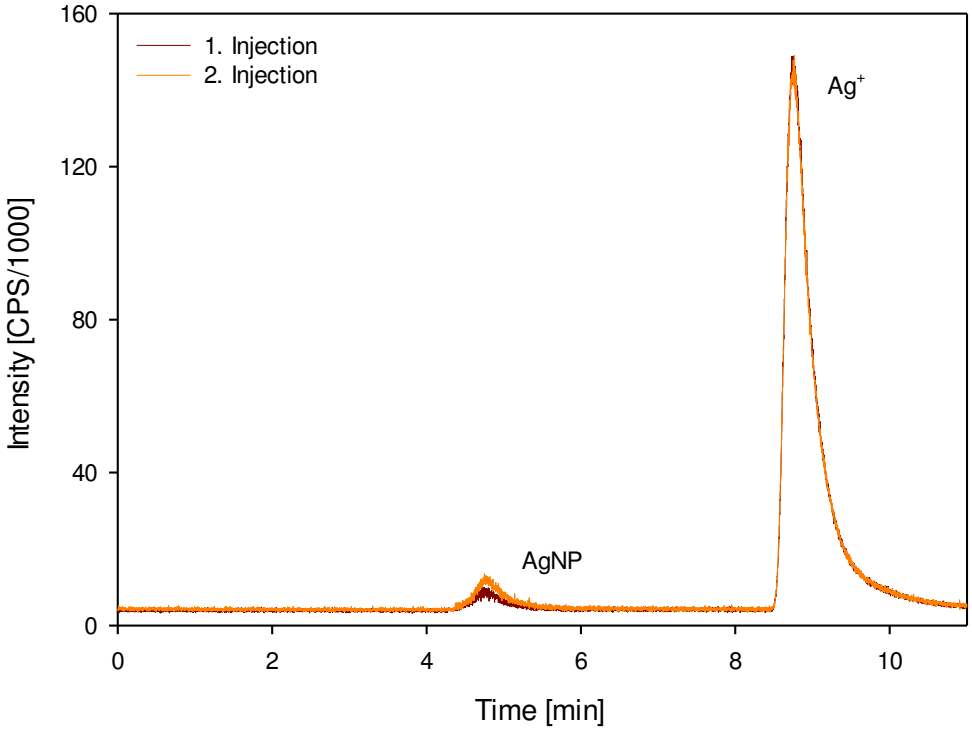


**Figure 17**: First two injections of a AgNP solution after covering the spray chamber with buffer solution for 3 hours, total silver amount of cit-AgNP solution: 130 µg/L Ag.

As it can be seen in the chromatograms above, also the conditioning of the spray chamber is unaccountable for reproducible cit-AgNP detection, because there was as always nearly no AgNP signal in the first two injections. Further the ionic silver peak was as always stable and strongly pronounced. But the factor time still played an important role, because the same sample was measured again after 6 hours without changing the setup and the results can be seen in Figure 18.

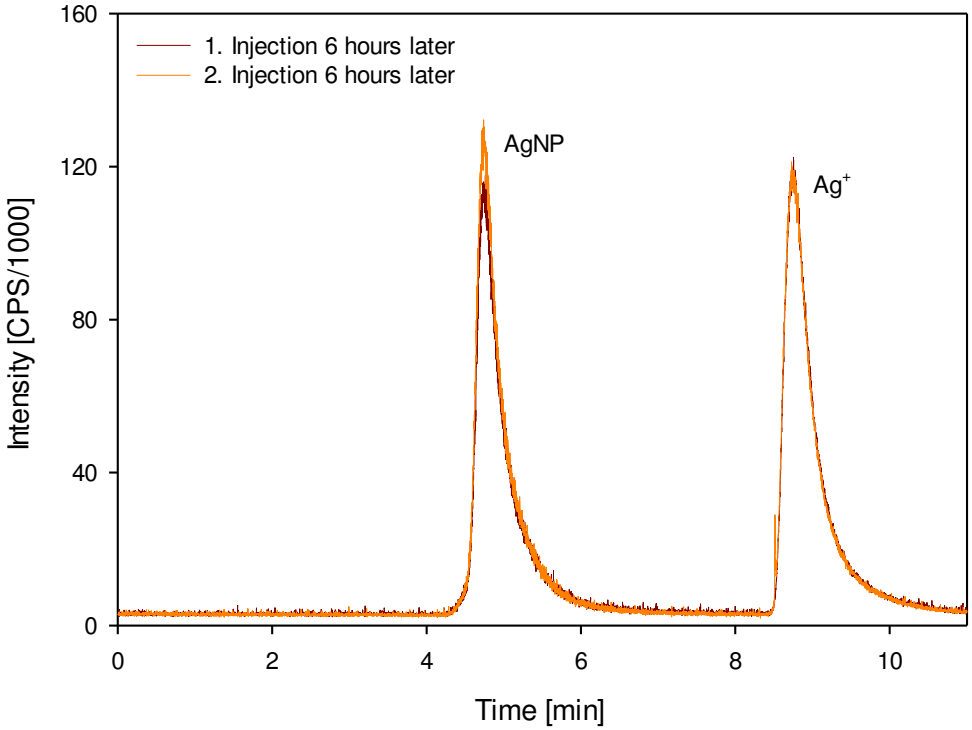


**Figure 18**: Massive increase of the measured AgNP content 6 hours after the sample was injected for the first time, total silver amount of cit-AgNP solution: 130 µg/L Ag.

A possible explanation for the previous results is, that probably the column has to be saturated with AgNPs to get a reproducible AgNP detection, because in the meantime many AgNP containing samples were injected on the column.

Experimental setup: HPLC 1260, ICPMS 7700x, TSK-GEL SUPERSW3000 column, flow rate 0.38 [mL/min].

### *3.4.4 Saturation of the TSK-GEL SUPERSW3000 column with AgNPs*

In the next experiment at first 10 injections of a just ionic silver containing sample were made to proof, that the separation of ionic silver is really reproducible (Figure 19). The reproducibility for 10 injections of a 100 µg/L ionic silver solution is really good: 2007 ± 22 [counts/1000].

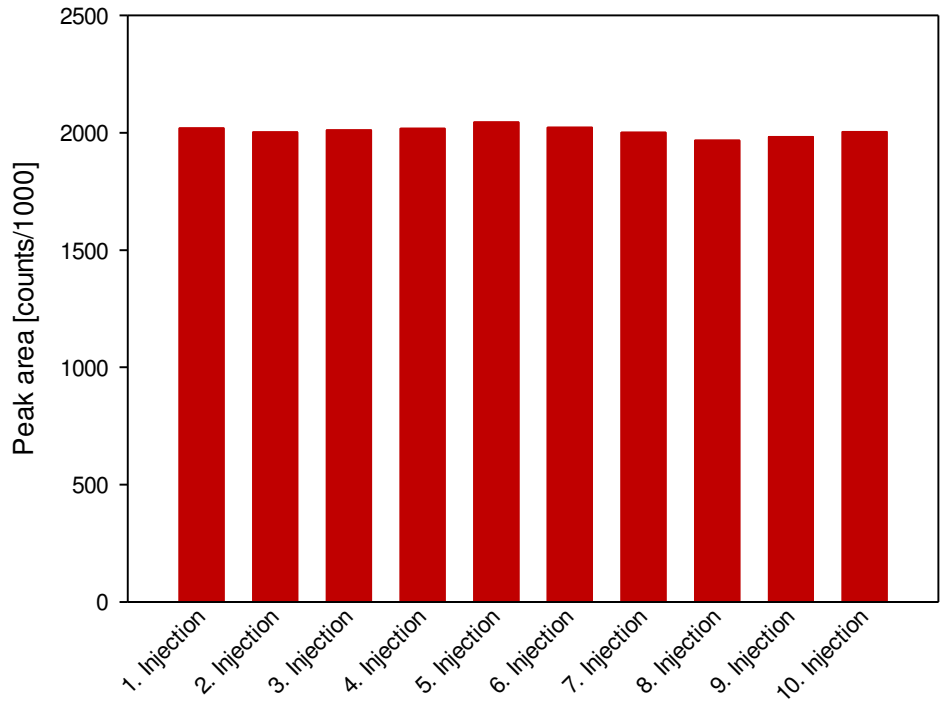


**Figure 19**: Reproducibility of a 100 µg/L ionic silver standard in buffer solution

Further 10 consecutive injections of the same cit-AgNP solution were made, followed by 10 injections of just buffer. Then again 10 injections of the same cit-AgNP solution as before were made. The 10 injections with the buffer only were made, because then just buffer flows through the column for 2 hours and maybe removes a part of the particles from the column and the column gets unsaturated from the AgNPs.

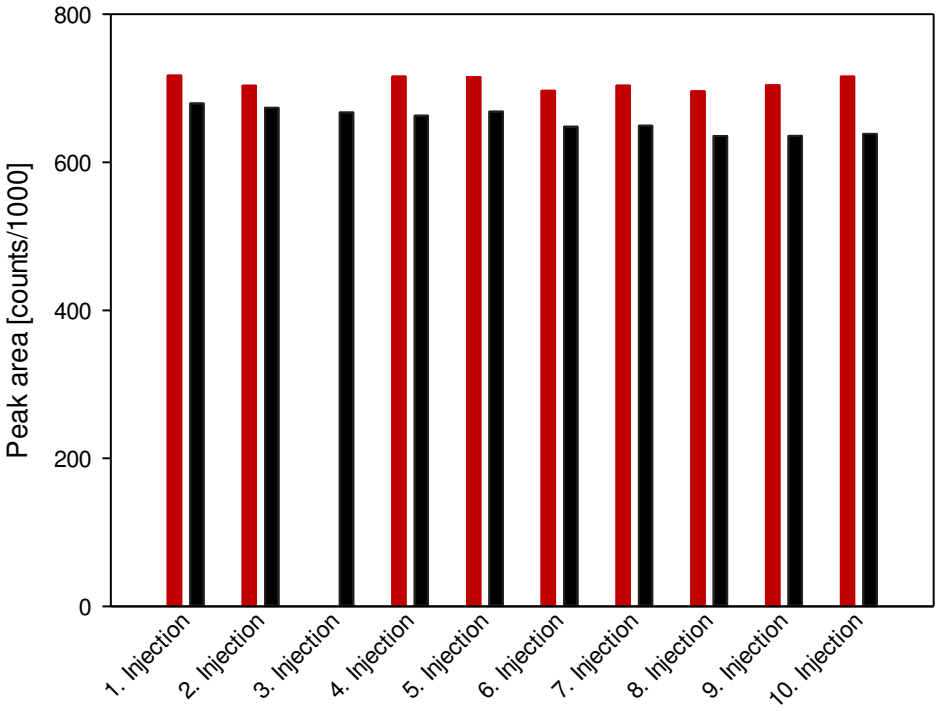


**Figure 20**: Reproducibility of the ionic silver concentration of a cit-AgNP solution with a total silver amount of 130 µg/L Ag, red bars – first 10 injections of the same cit-AgNP solution, black bars – further 10 injections of the same cit-AgNP solution after 10 buffer injections in between

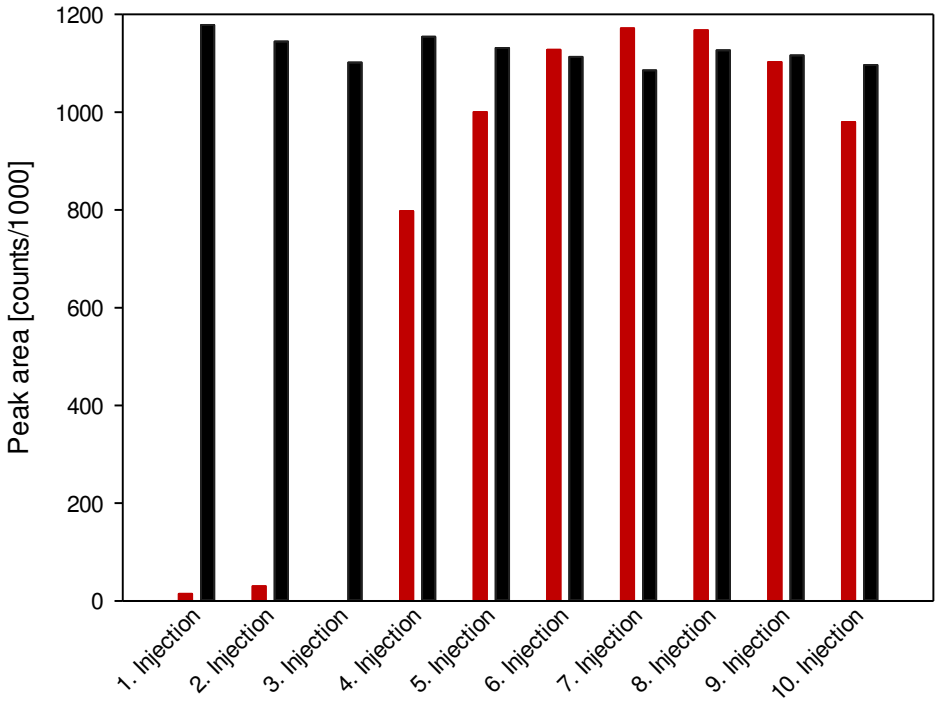


**Figure 21**: Reproducibility of the AgNP concentration of a cit-AgNP solution with a total silver amount of 130 µg/L Ag, red bars – first 10 injections of the same cit-AgNP solution, black bars – further 10 injections of the same cit-AgNP solution after 10 buffer injections in between

The results were quite promising this time. The signal for just the ionic silver concentration was quite stable and reproducible over all of the 20 injections of the same cit-AgNP solution (Figure 20). As it can be seen in Figure 21 there wasn't a AgNP signal at the first two injections, but then it was quite prominent. Also the possible saturation of the column with cit-AgNPs still looked very promising, because of the very reproducible AgNP signal. But the theory of the necessary column saturation was slightly undermined by the fact, that the 10 buffer injections in between weren't enough to remove the particles from the column.

To verify the hypothesis of the column saturation, a freshly prepared cit-AgNP solution was immediately injected with the same setup after the prior samples (Figure 22).

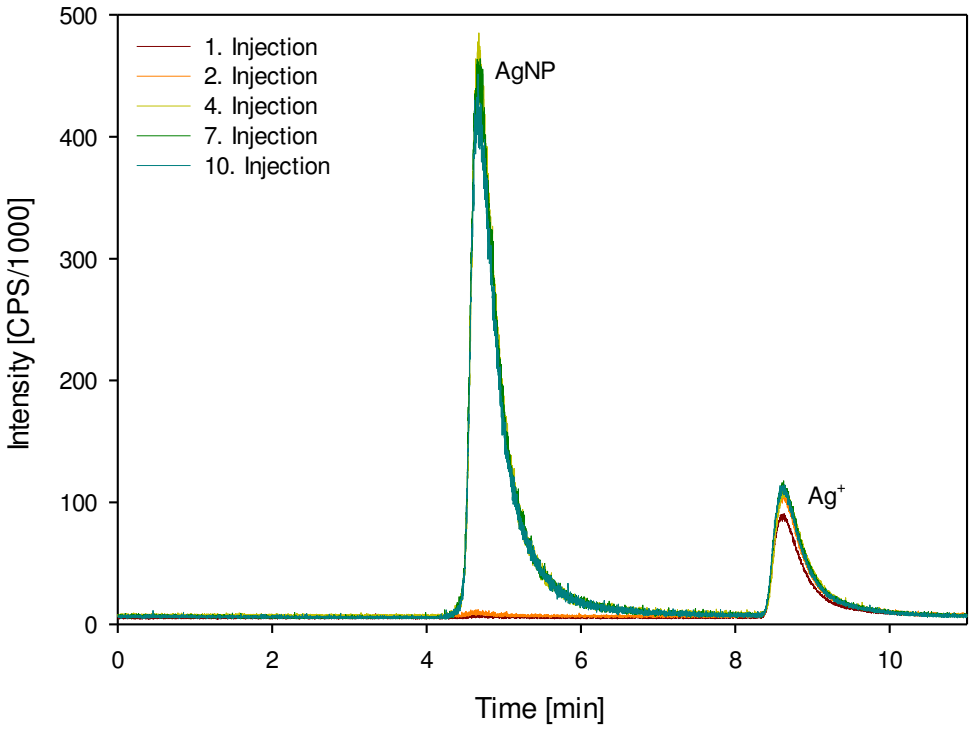


**Figure 22**: 10 injections of a fresh prepared AgNP solution after assumed saturation of the column with AgNPs, total silver amount of cit-AgNP solution: 130 µg/L Ag.

As a matter of fact, the possible saturation of the column was also not the reason for a reproducible AgNP detection, because with the fresh prepared cit-AgNP solution it was the same as usual. At the first two injections there was no AgNP signal, but then it increases.

Experimental setup: HPLC 1260, ICPMS 7700x, TSK-GEL SUPERSW3000 column, flow rate 0.38 [mL/min].

After these prior experiments, it was analyzed, which parameters are left to have an influence on the measurement of a cit-AgNP solution. The difference between the measurements of two samples which contain the exact same solution is the insertion of the HPLC needle and the HPLC needle puncturing the cap of the vial several times. Due to the puncturing maybe some crumbles fall into the AgNP solution and cause agglomeration of the AgNPs. Because of these reflections further experiments were done.

### *3.4.5 HPLC steel needle experiment*

In this experiment the influence of the HPLC steel needle on the AgNP solution was investigated. Therefore, the autosampler behavior was simulated. The experiment was done like this: insertion of the HPLC needle by hand in a fresh prepared cit-AgNP solution for 10 seconds, remove the needle, wait for 13 minutes, insert the needle in the same solution again for 10 seconds, remove the needle, wait for 13 minutes and then start the measurement of the sample with the HPLC-ICPMS. This experiment was done twice and the results can be seen in Figures 23 and 24.

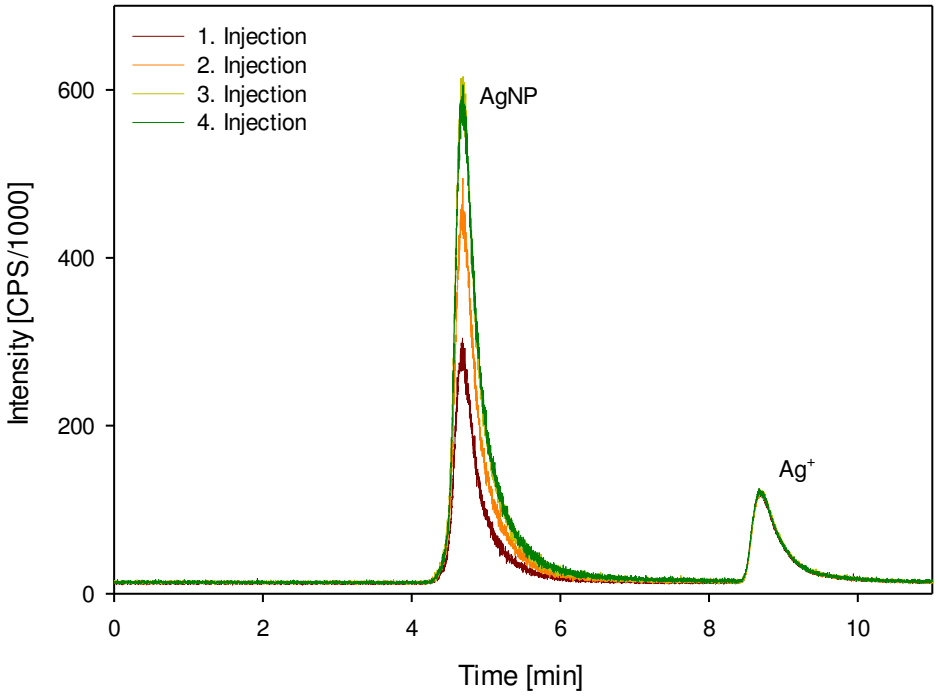


**Figure 23**: Chromatograms of a AgNP solution after an HPLC needle was inserted by hand two times, the autosampler behaviour was simulated for the first two injections, total silver amount of cit-AgNP solution: 130 µg/L Ag.

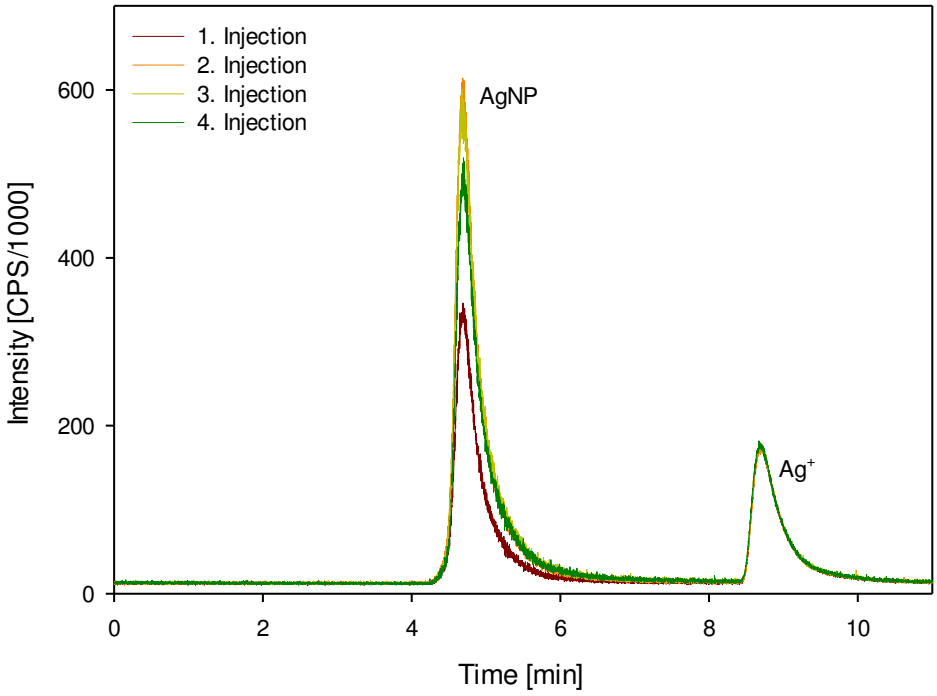


**Figure 24**: Chromatograms of a AgNP solution after an HPLC needle was inserted by hand two times, the autosampler behaviour was simulated for the first two injections, total silver amount of cit-AgNP solution: 130 µg/L Ag.

It is obvious from these results that the HPLC needle changes the cit-AgNP solution somehow and due to this, the AgNPs elute from the column and can be detected. But further measurements have to be done to really verify these results. Therefore one of the next experiments was conducted with a metal free HPLC system.

Experimental setup: HPLC 1260, ICPMS 7700x, TSK-GEL SUPERSW3000 column, flow rate 0.38 [mL/min].

### *3.4.6 Separation of cit-AgNPs from ionic silver with a C18 column*

For the next experiments the TSK-GEL SUPERSW3000 column was replaced with a C18 column. The experiment was performed to show whether the cit-AgNPs have the same behavior on the C18 column like on the TSK-GEL SUPERSW3000 column.

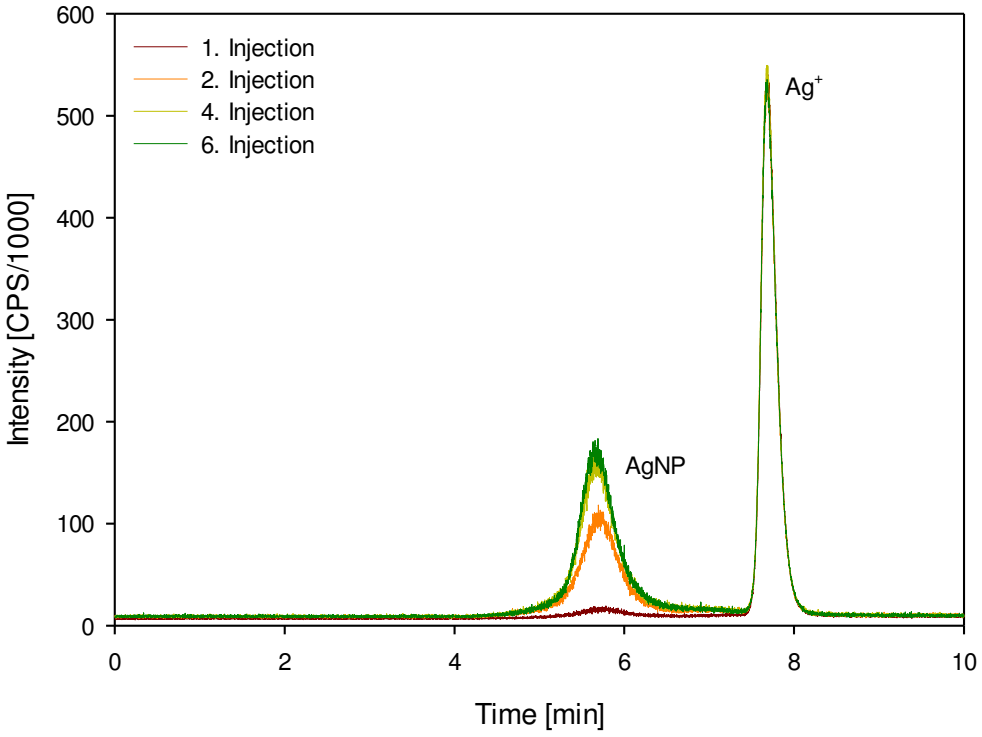


**Figure 25**: Chromatogram of the first injections of a AgNP solution on a C18 column, total silver amount of cit-AgNP solution: 130 µg/L Ag.

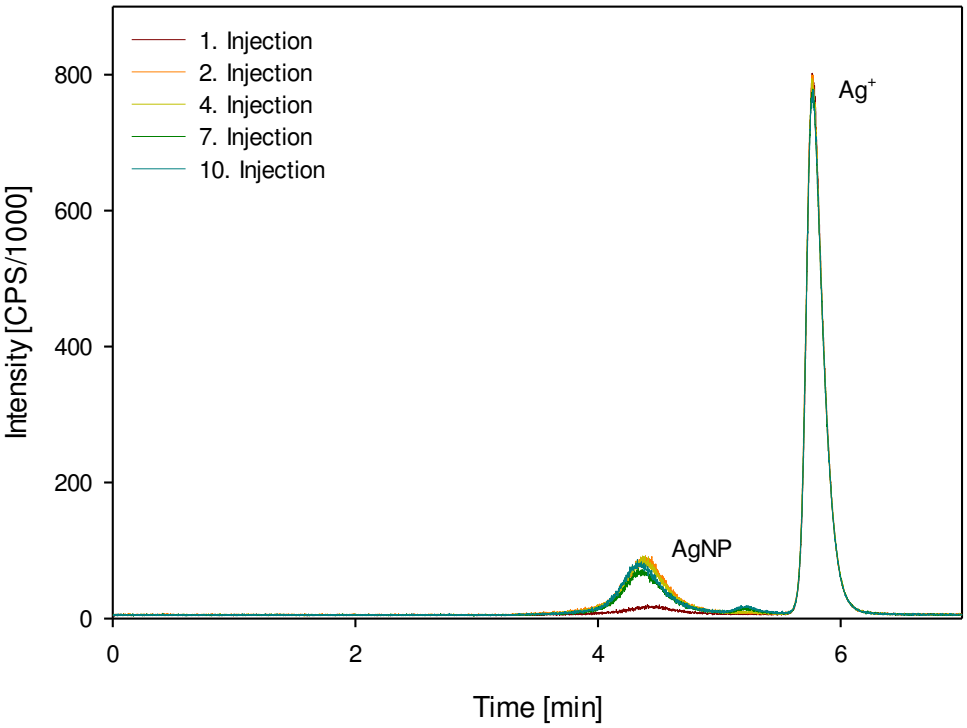


**Figure 26**: Chromatogram of 10 consecutive injections of a cit-AgNP solution on a C18 column with optimized run time, total silver amount of cit-AgNP solution: 130 µg/L Ag.

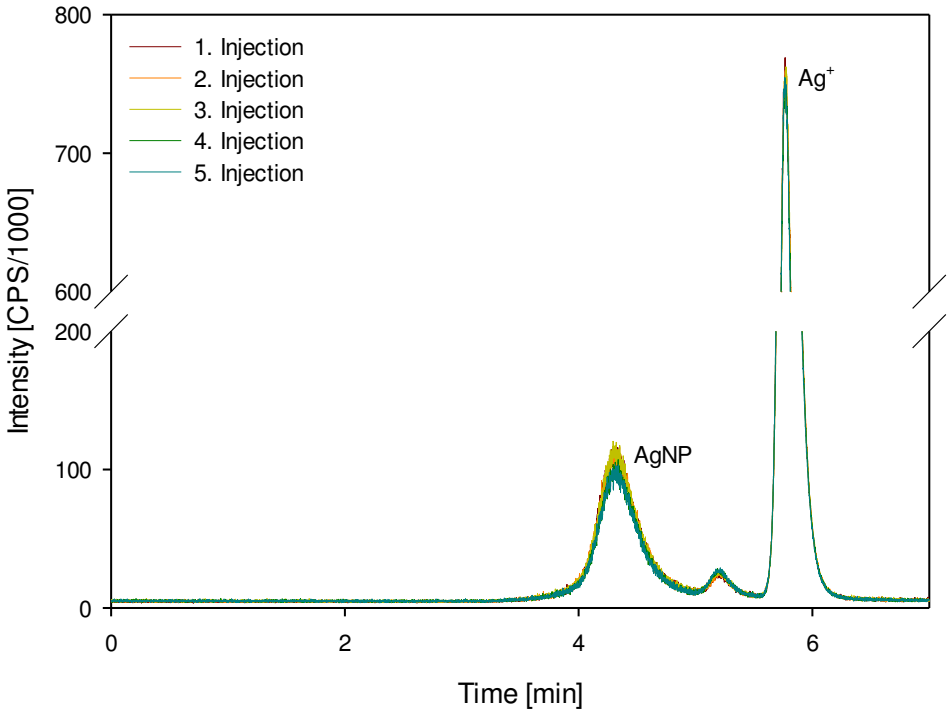


**Figure 27**: Chromatogram of 5 injections of the same cit-AgNP solution after 5 buffer injections with a small rising additional peak between the two big peaks, total silver amount of cit-AgNP solution: 130 µg/L Ag.

The first runs were done with a flow rate of 0.38 [mL/min] (Figure 25). Further on reproducibility runs were done with a higher flow rate of 0.50 [mL/min], what resulted in a shorter retention time, whereas the peaks are still baseline separated. Therefore 10 injections with cit-AgNPs (Figure 26) were made, followed by 5 injections of buffer and then another 5 injections of the same cit-AgNP solution were done (Figure 27). From this point of view the separation behavior is like on the TSK-GEL SUPERSW3000 column and also the phenomenon of the increasing AgNP signal and the stable ionic silver signal were observed. But as it can be seen in Figure 27 a small signal between the AgNP and ionic silver signals is rising.

Experimental setup: HPLC 1260, ICPMS 7700x, C18 column, flow rate 0.50 [mL/min].

### *3.4.7 Has the HPLC vial cap an influence on the increasing AgNP signal?*

As mentioned before maybe the cap of the vial has an influence on the increase of the AgNP signal. Because of this, an experiment without the cap on the vial was done. As it can be seen in Figure 28, the results were the same as the ones obtained for the closed vial (Figure 25). At the first two injections there is nearly no AgNP signal, but then it increases.

Experimental setup: HPLC 1260, ICPMS 7700x, C18 column, flow rate 0.50 [mL/min].

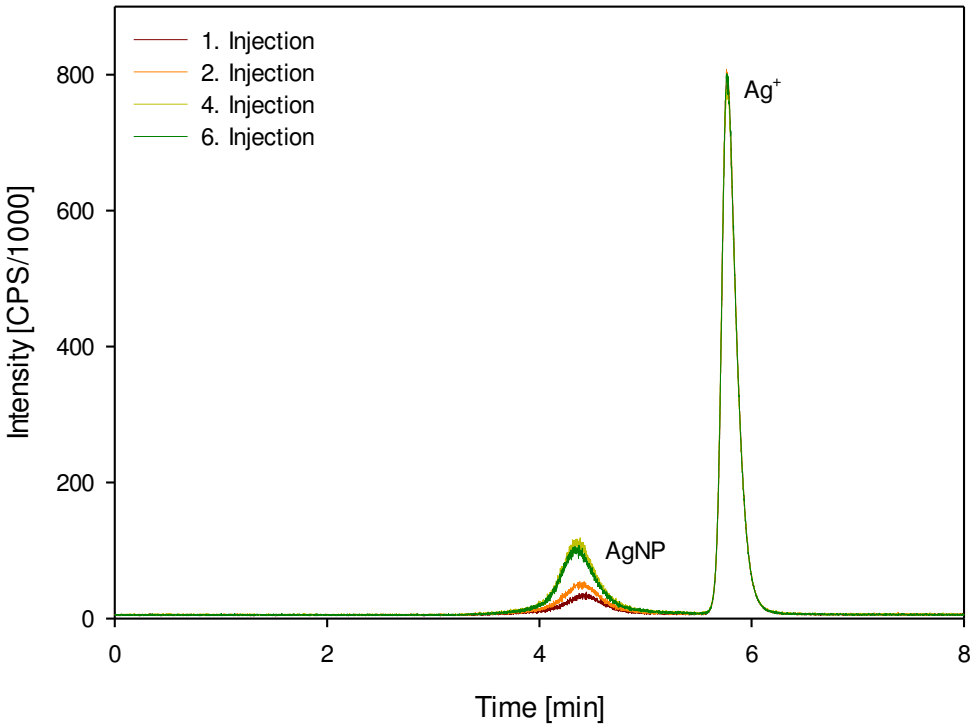


**Figure 28**: Chromatograms of a AgNP solution without HPLC vial cap, total silver amount of cit-AgNP solution: 130 µg/L Ag.

### *3.4.8 Measurement of cit-AgNPs with a metal free HPLC system*

To rule out the influence of the steel needle, an experiment with a metal free HPLC system was done. In total 15 consecutive injections of the same cit-AgNP solution were done. In the first 5 injections the AgNP signal was small and stable, but then the AgNP signal massively increased from one to another injection and was stable for further 10 injections (Figure 29).

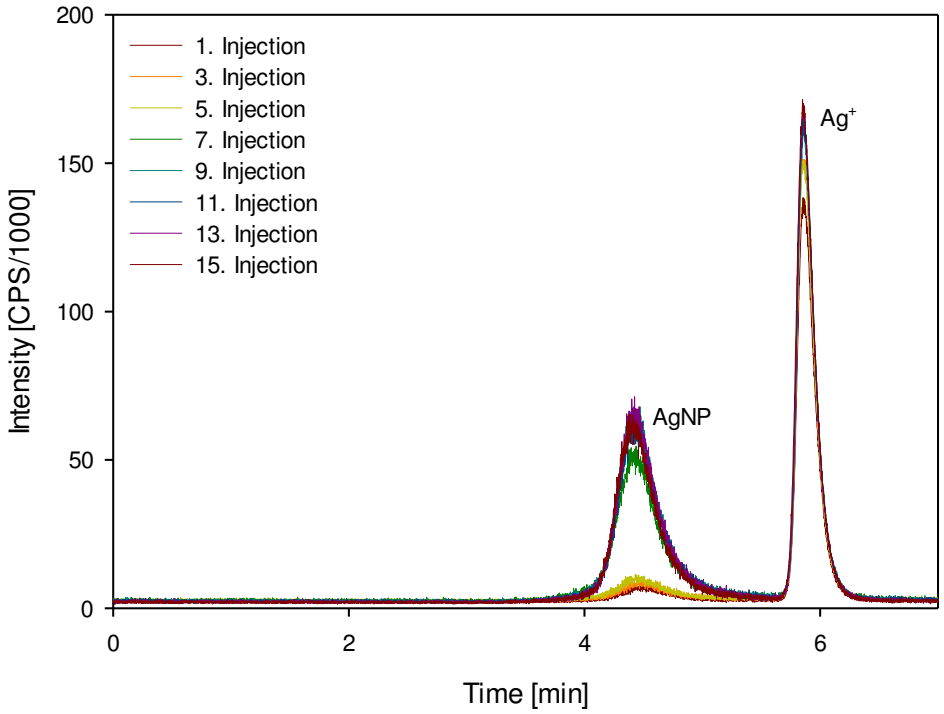


**Figure 29**: 15 consecutive injections of a AgNP solution with a metal free HPLC system, total silver amount of cit-AgNP solution: 130 µg/L Ag.

To verify this result the experiment was repeated once more. This time the sudden increase of the AgNP signal couldn't be observed. The AgNP signal slightly but constantly increased from injection to injection (Figure 30). As the results from the measurement with the metal free HPLC system weren't really reliable, the measurement should be repeated in the future to get a clearer view on the influence of the steel parts of a normal HPLC system on the measurement.

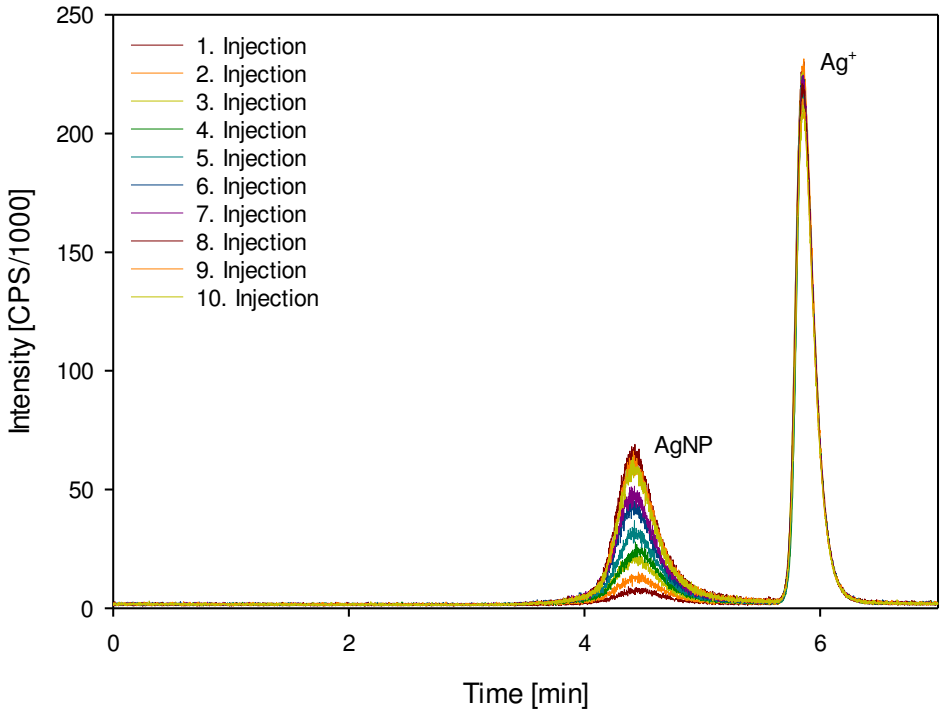


**Figure 30**: 10 injections of a AgNP solution with a metal free HPLC system, with a steady increasing AgNP peak, total silver amount of cit-AgNP solution: 130 µg/L Ag.

Experimental setup: metal free HPLC, ICPMS 7700x, C18 column, flow rate 0.50 [mL/min].

### *3.4.9 Attempt to reproduce the additional signal from Figure 27*

The next experiment was done to reproduce the small signal between the AgNP signal and the ionic silver signal as it was observed in an earlier experiment (Figure 27). Therefore 10 consecutive injections of the same cit-AgNP solution were done (Figure 31).

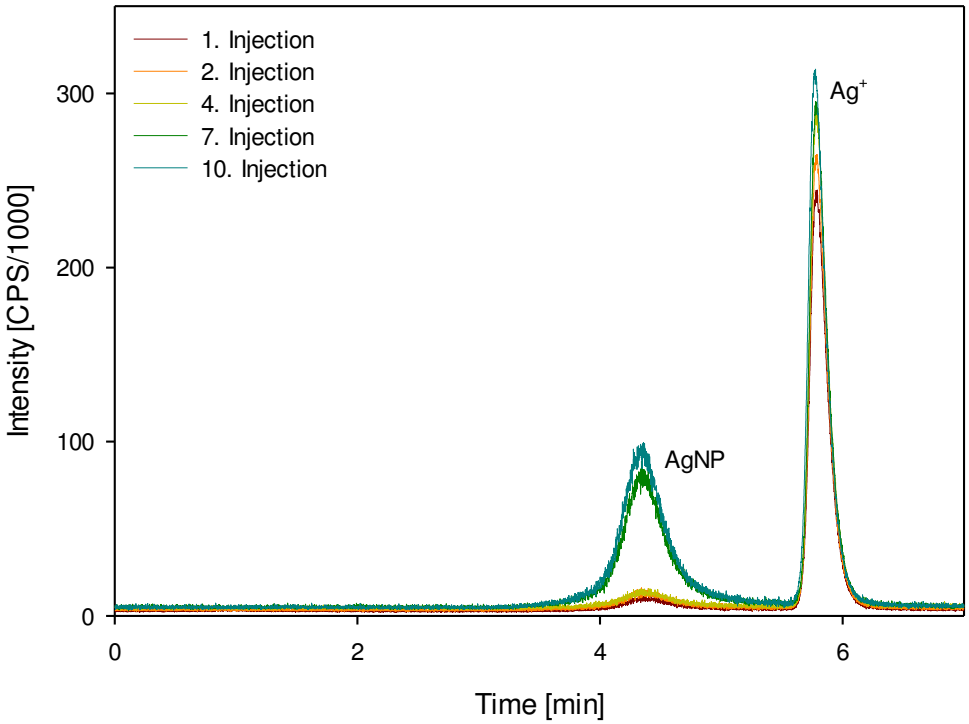


**Figure 31**: 10 injections of a AgNP solution, total silver amount of cit-AgNP solution: 130 µg/L Ag.

Surprisingly, this time not only the AgNP signal wasn't stable but also the ionic silver signal wasn't stable. Also in a second run of the same solution in another vial, both peaks weren't stable (Figure 32). Further the small signal between the AgNP signal and the ionic silver signal wasn't observed at all.

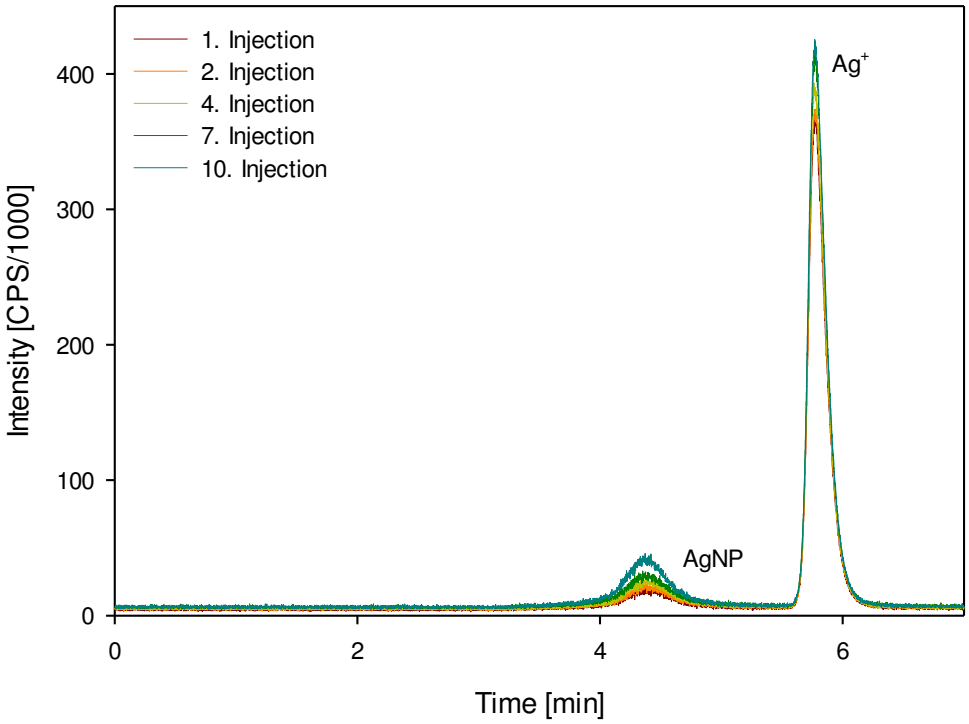


**Figure 32**: 10 injections of a cit-AgNP solution, total silver amount of cit-AgNP solution: 130 µg/L Ag.

Experimental setup: HPLC 1260, ICPMS 7700x, C18 column, flow rate 0.50 [mL/min].

### *3.4.10 Spiking of a cit-AgNP solution with ionic silver*

Because of the unstable ionic silver signal a spike experiment was performed. Therefore 5, 10, 15 and 20 µL of a 100 µg/L ionic silver containing solution were spiked to 20 µL of the ~130 µg/L Ag cit-AgNP solution. Figure 33 shows just 20 µL of the ionic silver solution, Figure 34 the cit-AgNP solution alone and with the various spikes. Each sample was injected 3 times and the reproducibility was good.

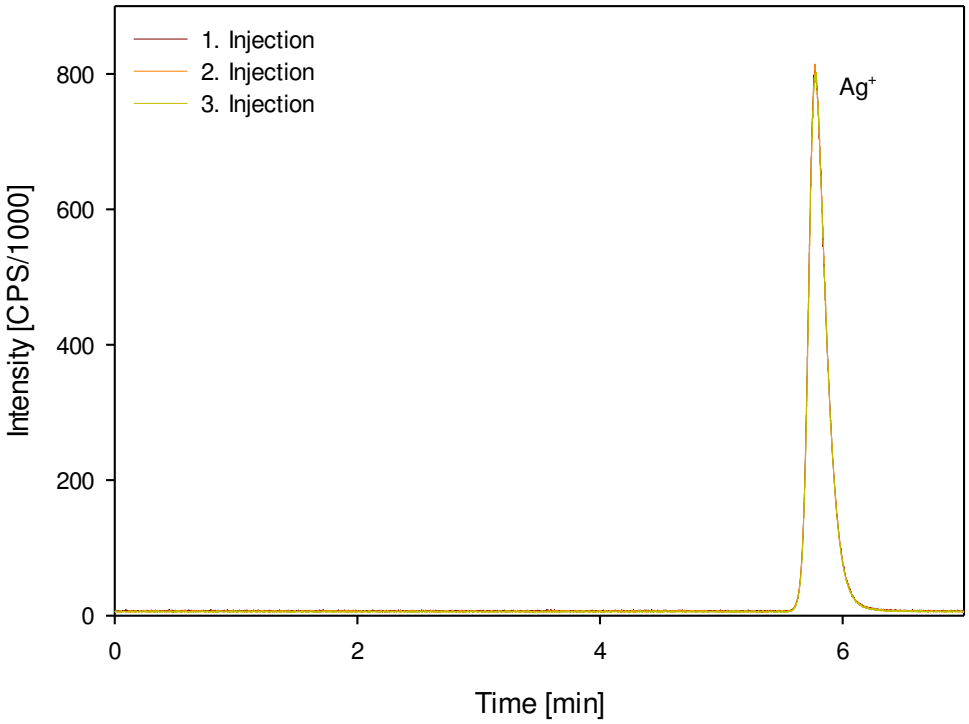


**Figure 33**: 3 injections of a 100 µg/L ionic silver containing solution

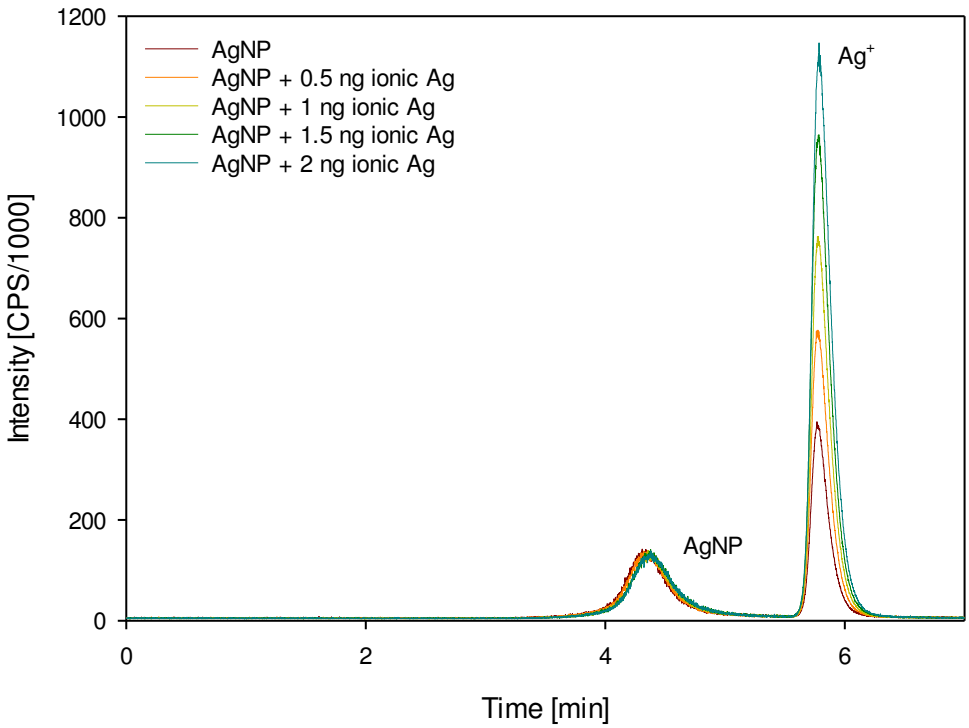


**Figure 34**: One injection each of a 10 hour old cit-AgNP solution alone and spiked with 0.5, 1, 1.5 and 2 ng of ionic silver

The recovery rate for the ionic fraction of the spiked solutions was around 100 %. The recovery rate was calculated by comparing the peak area from a flow injection measurement to the area obtained after C18 column separation.

Experimental setup: HPLC 1260, ICPMS 7700x, C18 column, flow rate 0.50 [mL/min].

### *3.4.11 Is there a linear correlation between the concentration and the peak area?*

The next question was if there is a linear behaviour between the sample concentration and the peak area. Therefore the cit-AgNP solution is once measured containing 130 µg/L Ag and once measured containing 65 µg/L Ag. As it can be seen in Figure 35 a linear correlation is not the case. Whether the combined areas (AgNP area + ionic silver area) correlate with the concentration nor the AgNP fraction or the ionic silver fraction. The measurement was performed just once.

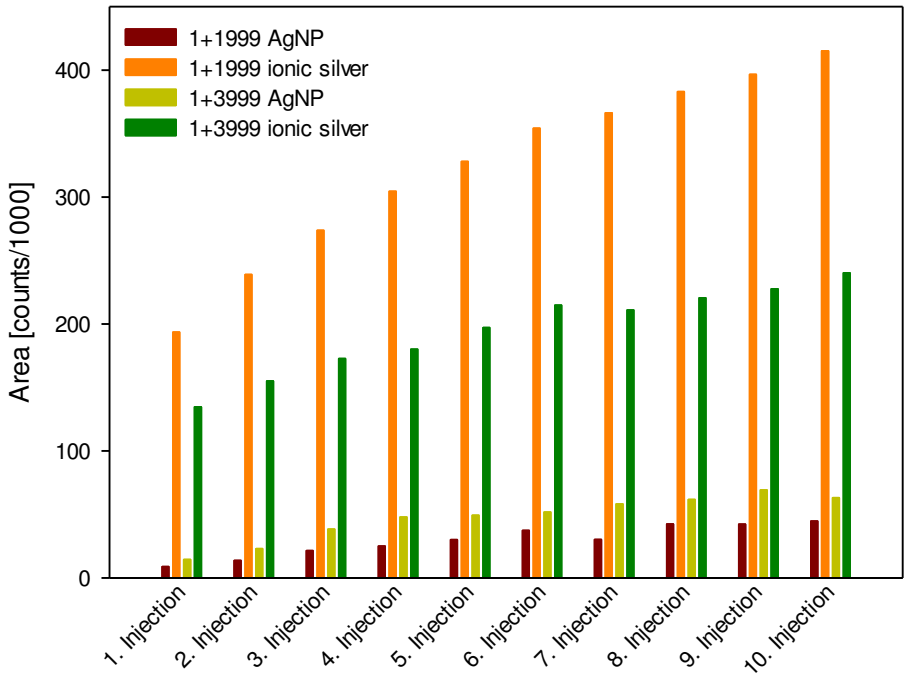


**Figure 35**: Comparison of a cit-AgNP solution containing ~130 µg/L Ag with a cit-AgNP solution containing just ~ 65 µg/L Ag

Experimental setup: HPLC 1260, ICPMS 7700x, C18 column, flow rate 0.50 [mL/min].

### *3.4.12 Is the measured concentration the same, if the same cit-AgNP solution is divided into several vials?*

In the process of the last experiments another important observation was made. When the same cit-AgNP solution is divided into 3 different vials and subsequently measured, different results for the AgNP signal and the ionic silver signal were obtained (Figure 36 and Table 6).

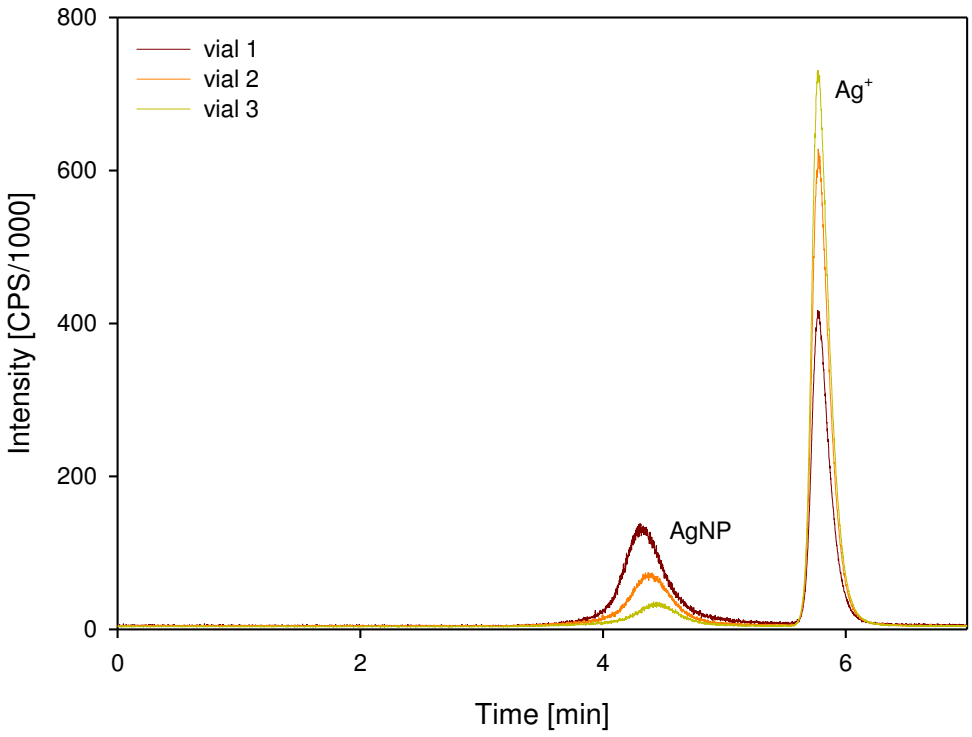


**Figure 36:** Chromatograms of the same cit-AgNP solution divided in 3 vials, total silver amount of cit-AgNP solution: 130 µg/L Ag.

**Table 6**: Concentrations of the AgNP fraction and the ionic silver fraction of a 130 µg/L Ag AgNP solution, which is divided into 3 different vials for measurement

| | AgNP Area [counts] | Ionic silver Area [counts] | Sum of areas [counts] |
|---|---|---|---|
| **cit-AgNP vial 1** | 295000 | 429000 | 724000 |
| **cit-AgNP vial 1** | 295000 | 418000 | 713000 |
| **cit-AgNP vial 1** | 306000 | 422000 | 728000 |
| **cit-AgNP vial 2** | 161000 | 648000 | 809000 |
| **cit-AgNP vial 2** | 157000 | 653000 | 810000 |
| **cit-AgNP vial 2** | 156000 | 650000 | 806000 |
| **cit-AgNP vial 3** | 65000 | 753000 | 818000 |
| **cit-AgNP vial 3** | 65000 | 774000 | 839000 |
| **cit-AgNP vial 3** | 54000 | 770000 | 824000 |

Until now there was no reason found why the results differ dramatically for the inter vial comparison, but the measurement was performed just once, so it has to be repeated in the future.

Experimental setup: HPLC 1260, ICPMS 7700x, C18 column, flow rate 0.50 [mL/min].

### *3.4.13 Determination of the ionic silver concentration of a cit-AgNP solution with the standard addition method*

The ionic silver concentration of a cit-AgNP solution was determined with the standard addition method. Therefore the cit-AgNP solution was spiked with 25, 50, 100 and 150 µg/L ionic silver and only the ionic silver peak was integrated in the chromatograms. The determined ionic silver concentration was ~ 20 µg/L. The result can be seen in Figure 37.

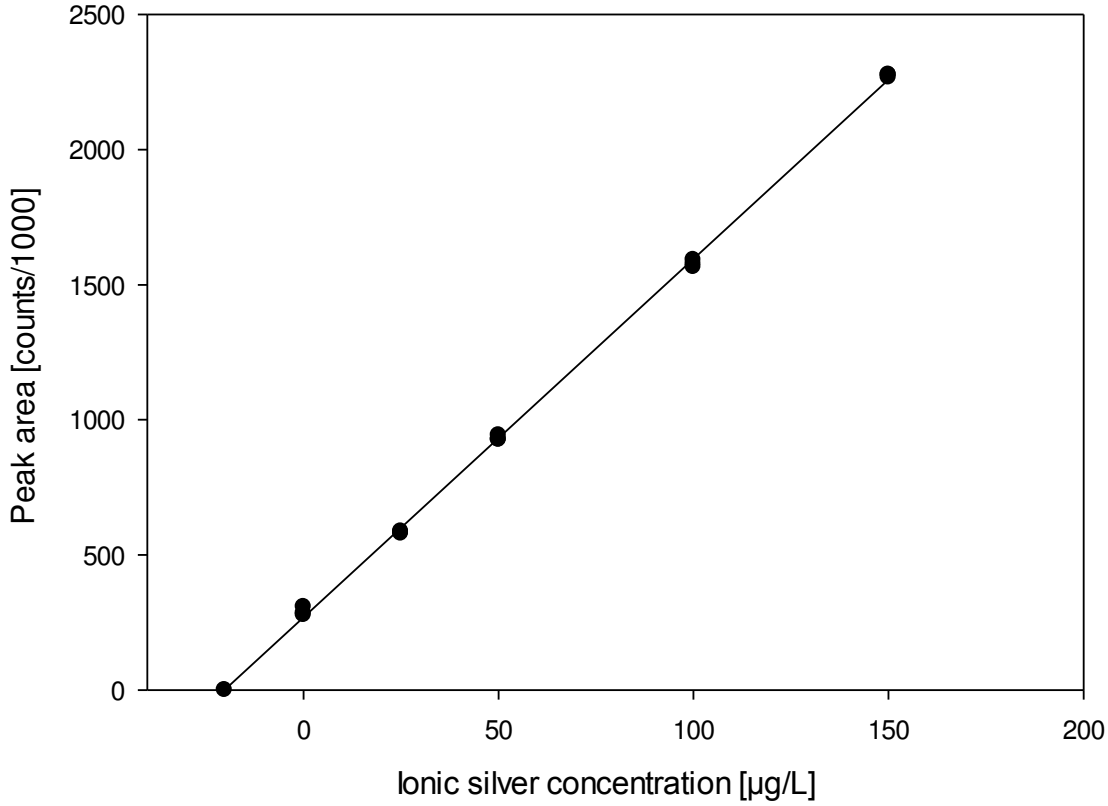


**Figure 37**: Determination of the ionic silver concentration of a cit-AgNP solution with the standard addition method using HPLC-ICPMS

Experimental setup: HPLC 1260, ICPMS 7700x, C18 column, flow rate 0.50 [mL/min].

For the determination of the total silver content of the before mentioned cit-AgNP solution the column was removed and flow injection analysis was done. The total silver concentration of the cit-AgNP solution of ~77 µg Ag/L was determined with the help of the standard addition method (see Figure 38). Thus the ionic silver fraction of the cit-AgNP solution is ~ 23%.

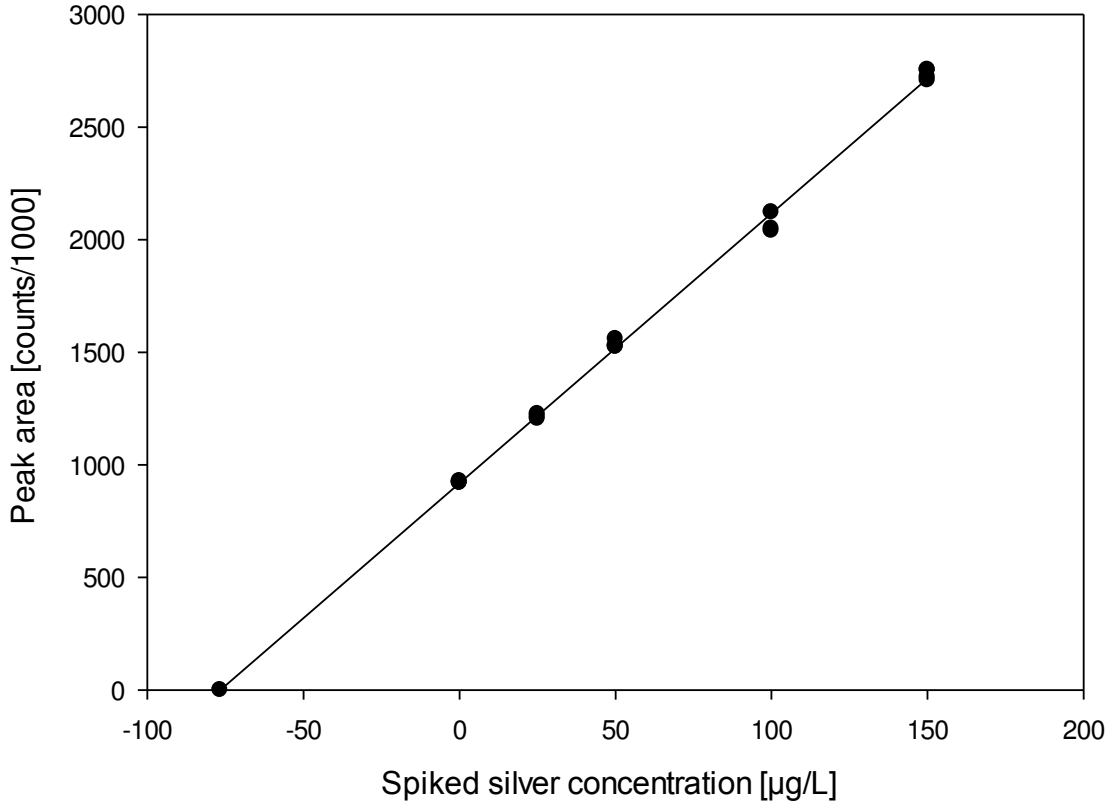


**Figure 38**: Determination of the total silver concentration of a cit-AgNP solution with the standard addition method using flow injection HPLC-ICPMS analysis

Experimental setup: HPLC 1260, ICPMS 7700x, no column, flow rate 0.50 [mL/min].

### *3.4.14 Measurement of ionic silver standards with HPLC-ICPMS*

But when just ionic silver solutions (25, 50, 100, 130 and 150 µg Ag/L) were measured with this HPLC-ICPMS method the column recovery is between 125 and 130 % (see Table 7). Right now there was no reason found, for the too high column recovery.

**Table 7**: Column recovery of various ionic silver standard concentrations

| Ag concentration [µg/L] | Flow injection peak area [counts] | Column peak area [counts] | Column recovery [%] |
|---|---|---|---|
| 25 | 277000 | 353000 | 127 |
| 50 | 549000 | 700000 | 128 |
| 100 | 1097000 | 1390000 | 127 |
| 130 | 1392000 | 1780000 | 128 |
| 150 | 1627000 | 2100000 | 129 |

Experimental setup: HPLC 1260, ICPMS 7700x, C18 column, flow rate 0.50 [mL/min].

### 3.5 Single particle ICPMS measurements

The measurements with sp-ICPMS were done with an Agilent 7700x ICPMS and as Software the MassHunter Workstation Single Nanoparticle Application Module was used.

For the calibration following samples were needed: a blank, which is just containing ultrapure water (Figure 39), a 1 µg/L ionic silver in ultrapure water solution (Figure 40) and a AgNP containing solution (Figure 41). The cit-AgNP solution was diluted with ultrapure water to a final concentration of 0.52 µg/L Ag. All solutions were prepared in PP-HPLC vials. For the measurement the 0.52 µg/L Ag containing cit-AgNP solution was further spiked with 0.1, 0.25, 0.5, 0.75 and 1 µg/L ionic silver (Figure 42).

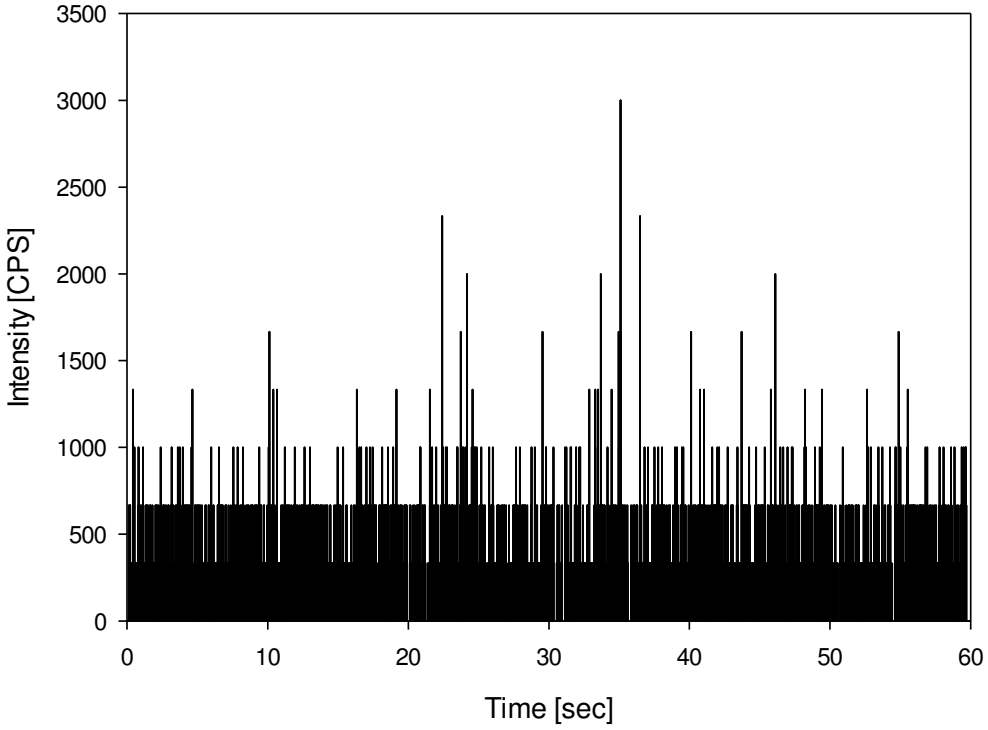


**Figure 39**: Time Scan chart of an ultrapure water blank

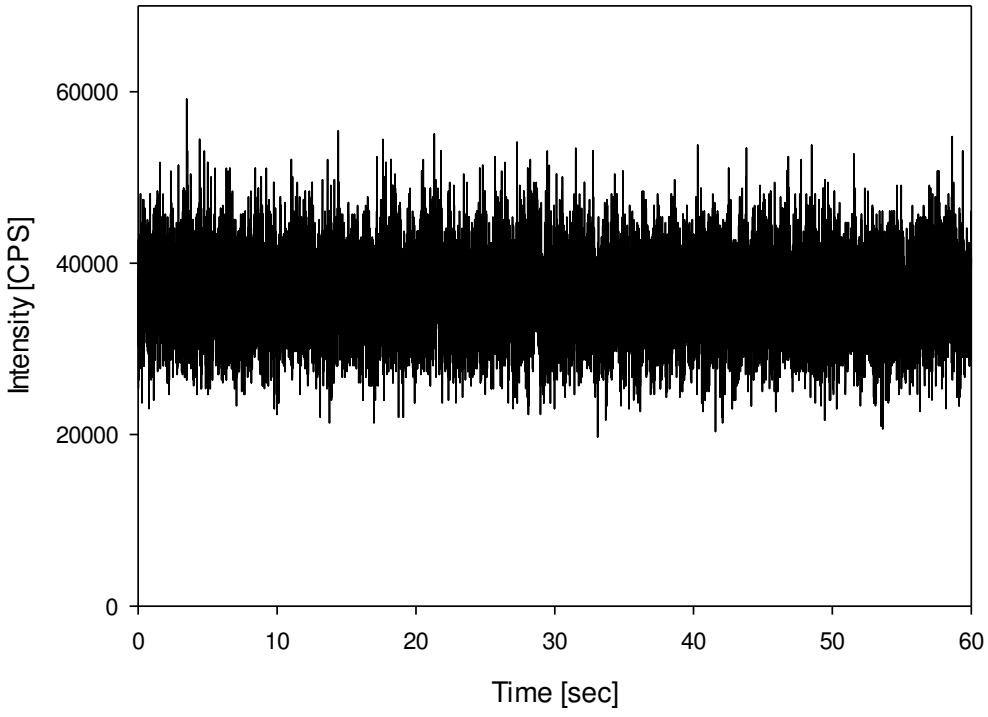


**Figure 40**: Time Scan chart of a 1 µg/L Ag solution

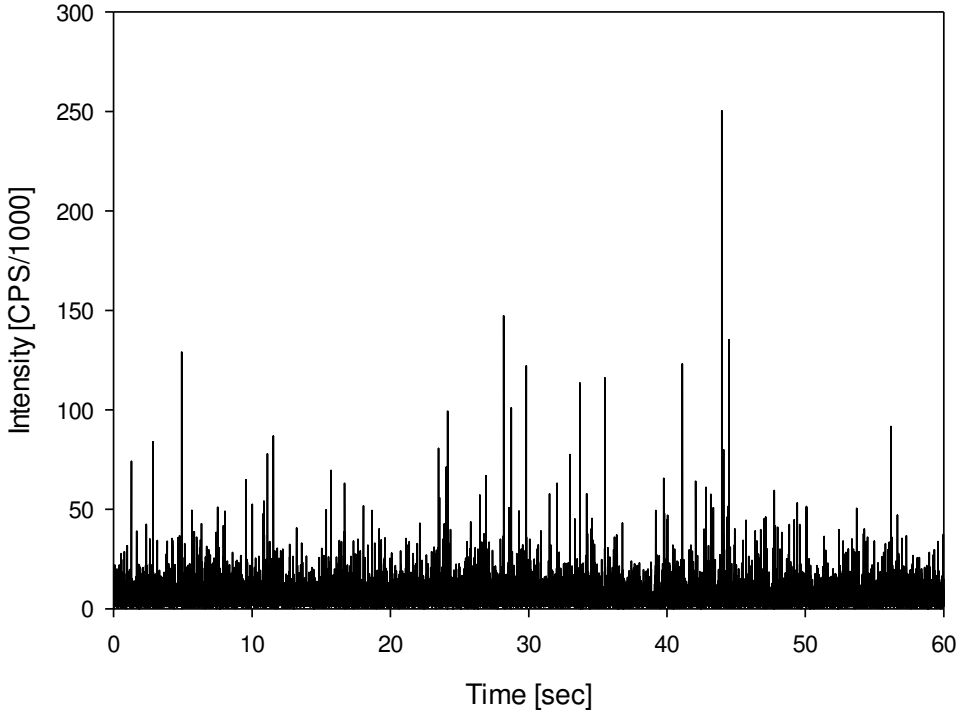


**Figure 41**: Time Scan chart of a cit-AgNP solution with a concentration of 0.52 µg/L Ag

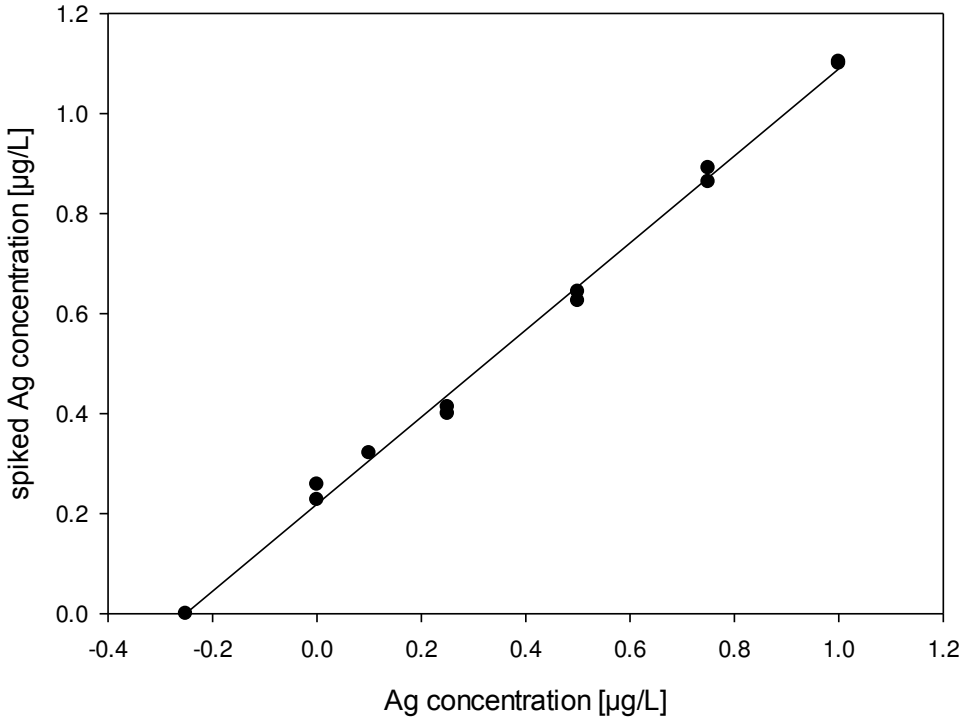


**Figure 42**: With the standard addition method determined ionic silver concentration of a cit-AgNP solution using sp-ICPMS

In this spike experiment the determined concentration of ionic silver in the 0.52 µg/L Ag containing cit-AgNP solution is 0.25 µg Ag/L. So according to this the ionic silver fraction is ~48 %.

But when cit-AgNPs were measured less diluted, the ionic silver fraction increases from 48 % to 65 %, as it can be seen in Table 8.

**Table 8**: Determined amount of ionic silver in cit-AgNP solutions with various concentrations

| total Ag in cit-AgNP solution [µg/L] | ionic silver concentration [µg/L] | ionic silver [%] |
|---|---|---|
| 0.52 | 0.23 | 44 |
| 0.52 | 0.26 | 50 |
| 13.2 | 7.93 | 60 |
| 13.2 | 7.95 | 60 |
| 26.4 | 17.09 | 65 |
| 26.4 | 17.44 | 66 |

It is further very interesting that although a 1 µg/L ionic silver solution is needed for calibration, the software returns a silver concentration of 0.9 µg/L, when the standard is remeasured as a sample (see Table 9).

**Table 9**: Determined ionic silver concentration of a 1 µg/L Ag solution

| intended ionic silver concentration [µg/L] | determined ionic silver concentration [µg/L] |
|---|---|
| 1 | 0.90 |
| 1 | 0.90 |
| 1 | 0.90 |
| 1 | 0.91 |
| 1 | 0.89 |
| 1 | 0.89 |

Also when elements like Li, Y and Tl with a concentration of 1 µg/L are measured with sp-ICPMS, first as ionic standard and then the same solution as sample, the determined concentration is always 5 – 10 % too low (Table 10).

**Table 10**: Determined ionic concentration of a 1 µg/L Li, Y and Tl solution

| intended ionic concentration [µg/L] | determined Li [µg/L] | determined Y [µg/L] | determined Tl [µg/L] |
|---|---|---|---|
| 1 | 0.92 | 0.94 | 0.95 |
| 1 | 0.93 | 0.93 | 0.95 |
| 1 | 0.93 | 0.93 | 0.95 |
| 1 | 0.93 | 0.94 | 0.95 |

# 4 Conclusions & Outlook

All in all it can be said, that the separation of silver nanoparticles from ionic silver is possible, independent from the used column. Right now this method can just be used to obtain qualitative information, whether a sample is containing AgNPs and/or silver ions. Before this method can be used, for the quantification of silver containing samples, the severe reproducibility problems have to be overcome. Further this method has then to be tested, if the separation of AgNPs of different sizes is also possible, like in the original method from Soto-Alvaredo.

The comparison of the HPLC-ICPMS method with sp-ICPMS is difficult, because the results for the amount of ionic silver in a cit-AgNP solution differ dramatically between the two methods. For sp-ICPMS analysis of the cit-AgNP solution, the ionic silver concentration ranged from 44 % to 65 % depending on dilution. Further the determined silver concentration of a 1 µg/L ionic silver solution was just 0.9 µg Ag/L, although the same solution was used for calibration. For the HPLC-ICPMS method the determined ionic silver concentration in a cit-AgNP solution was just about 23 %. When only ionic silver is measured with the RP-HPLC-ICPMS method, the column recovery is 130 %. So both methods have difficulties to reliably determine the ionic silver content of a cit-AgNP solution or in an ionic silver solution. Right now it can't be said, which method is the more reliable one.

Despite the fact that there are still problems with the reliable determination of the ionic silver content, both methods have a major drawback: the AgNP containing solutions have to be diluted prior to measurement. That's why it can't be said, if the determined amount of ionic silver is already present in the original sample, or if it is a result of the sample preparation, because of the dissolution of the AgNPs.

For the future there are a few things which can be done again or some other parameters which can be looked at. For example, the measurement with the metal free-HPLC system definitely has to be repeated. The two performed measurements just gave erratic results which raised more questions than they

answered. Therefore this method has to be checked again, if it still gives erratic results, which couldn’t be explained in the first place.

Further a cyclonic spray chamber could be tested instead of a Scott spray chamber. Maybe the reduced spray chamber volume results in a better transport efficiency of the AgNPs to the plasma. Also an inert spray chamber could be tested, if it has any influence on the measurement reproducibility. Another possibility would be to test an inert column material. Maybe the silver species interact with the steel column which leads to the reproducibility problems.

Due to the fact that there are still some parameters left to be tested, there is still the possibility that the reliability problems can be solved in the future.

# 5 Abbreviations

*E. coli* – *Escherichia coli*

*S. aureus* – *Staphylococcus aureus*

*V. cholerae* – *Vibrio cholerae*

*P. aeruginosa* – *Pseudomonas aeruginosa*

SDS – Sodium dodecyl sulfate

AgNPs – silver nanoparticles

PEG – polyethylene glycol

ROS – reactive oxygen species

SEM – scanning electron microscopy

PCi – post column injection

EDS – energy dispersive spectroscopy

TEM – transmission electron microscopy

SEC – size exclusion chromatography

HPLC – high performance liquid chromatography

ICPMS – inductively coupled plasma mass spectrometry

DLS – dynamic light scattering

sp-ICPMS – single particle ICPMS

AF4 – asymmetrical flow field flow fractionation

RP-HPLC-ICPMS – reversed phase HPLC-ICPMS

CPE – cloud point extraction

HDC – hydrodynamic chromatography

IBAD – ion beam assisted deposition

LoVo – human colon carcinoma cell line

AgAc – silver acetate

PVP – polyvinylpyrrolidone

PVA – polyvinyl alcohol

ROS – reactive oxygen species

PEG – polyethylene glycol

MES – mouse embryonic stem cells

MEF – mouse embryonic fibroblasts

NTA – nanoparticle tracking analysis

CF3 – centrifugal field-flow fractionation

F-AAS – flame atomic absorption spectrometry

CTAB – cetyl trimethylammonium bromide

PEEK – polyether ether ketone

# 6 References

[1] Wiberg, H. Lehrbuch der Anorganischen Chemie, 101st ed.; *deGruyter,* **1995.**

[2] Russell, A. D., Hugo, W. B. edited by Ellis, G. P. and Luscombe, D. K. Progress in Medicinal Chemistry*:* Antimicrobial Activity and Action of Silver; *Elsevier Science B.V.,* **1994.**

[3] Chaloupka, K.; Malam, Y.; Seifalian, A. M. Nanosilver as a new generation of nanoproduct in biomedical applications. *Trends Biotechnol.* **2010,** 28, 580–588.

[4] Davies, R.L.; Etris, Samuel F. The development and functions of silver in water purification and disease control. *Catal. Today* **1997,** 36, 107–114.

[5] Nelson, D.L.; Cox, M. M. Lehninger Principles of Biochemistry, 6th ed.; *W. H. Freeman,* **2013.**

[6] Feng, Q. L.; Wu, J.; Chen, G. Q.; Cui, F. Z.; Kim, T. N.; Kim, J. O. A mechanistic study of the antibacterial effect of silver ions on Escherichia coli and Staphylococcus aureus. *J. Biomed. Mater. Res.* **2000,** 52, 662–668.

[7] Jung, W. K.; Koo, H. C.; Kim, K. W.; Shin, S.; Kim, S. H.; Park, Y. H. Antibacterial activity and mechanism of action of the silver ion in Staphylococcus aureus and Escherichia coli. *Appl. Environ. Microb.* **2008,** 74, 2171–2178.

[8] Klueh, U.; Wagner, V.; Kelly, S.; Johnson, A.; Bryers, J. D. Efficacy of silver-coated fabric to prevent bacterial colonization and subsequent device-based biofilm formation. **2000,** 53, 621–631.

[9] THE EUROPEAN COMMISSION. Commission Recommendation of 18 October 2011 on the definition of nanomaterial. *OJ L275/38* **2011,** 38–40.

[10] http://www.nanosilver.it/ted/applicazioni.htm, (accessed Dec 11, 2014).

[11] Verano-Braga, T.; Miethling-Graff, R.; Wojdyla, K.; Rogowska-Wrzesinska, A.; Brewer, J. R.; Erdmann, H.; Kjeldsen, F. Insights into the Cellular Response Triggered by Silver Nanoparticles Using Quantitative Proteomics. *ACS Nano* **2014,** 8, 2161–2175.

[12] Loeschner, K.; Hadrup, N.; Qvortrup, K.; Larsen, A.; Gao, X.; Vogel, U.; Mortensen, A.; Lam, H.; Larsen, E. H. Distribution of silver in rats following 28 days of repeated oral exposure to silver nanoparticles or silver acetate. *Part. Fibre Toxicol.* **2011,** 8, 1–14.

[13] Ribeiro, F.; Gallego-Urrea, J. A.; Jurkschat, K.; Crossley, A.; Hassellöv, M.; Taylor, C.; Soares, A. M.; Loureiro, S. Silver nanoparticles and silver nitrate induce high toxicity to Pseudokirchneriella subcapitata, Daphnia magna and Danio rerio. *Sci. Total Environ.* **2014,** 266–267, 232–241.

[14] Choi, O.; Deng, K. K.; Kim, N.-J.; Ross, L.; Surampalli, R. Y.; Hu, Z. The inhibitory effects of silver nanoparticles, silver ions, and silver chloride colloids on microbial growth. *Water Res.* **2008,** 42, 3066–3074.

[15] Xiu, Z.-M.; Ma, J.; Alvarez, P. J. J. Differential Effect of Common Ligands and Molecular Oxygen on Antimicrobial Activity of Silver Nanoparticles versus Silver Ions. *Environ. Sci. Technol.* **2011,** 45, 9003–9008.

[16] Sotiriou, G. A.; Pratsinis, S. E. Antibacterial Activity of Nanosilver Ions and Particles. *Environ. Sci. Technol.* **2010,** 44, 5649–5654.

[17] Xiu, Z.-M.; Zhang, Q.-B.; Puppala, H. L.; Colvin, V. L.; Alvarez, P. J. J. Negligible Particle-Specific Antibacterial Activity of Silver Nanoparticles. *Nano Lett.* **2012,** 12, 4271–4275.

[18] Lok, C.-N.; Ho, C.-M.; Chen, R.; He, Q.-Y.; Yu, W.-Y.; Sun, H.; Tam, P.K.-H.; Chiu, J.-F.; Che, C.-M. Silver nanoparticles: partial oxidation and antibacterial activities. *J. Biol. Inorg. Chem.* **2007,** 12, 527–534.

[19] Morones, J. R.; Elechiguerra, J. L.; Camacho, A.; Holt, K.; Kouri, J. B.; Ramírez, J. T.; Yacaman, M. J. The bactericidal effect of silver nanoparticles. *Nanotechnology* **2005,** 16, 2346–2353.

[20] Sondi, I.; Salopek-Sondi, B. Silver nanoparticles as antimicrobial agent: a case study on E. coli as a model for Gram-negative bacteria. *J. Colloid Interface Sci.* **2004,** 275, 177–182.

[21] Lee, K. J.; Nallathamby, P. D.; Browning, L. M.; Osgood, C. J.; Xu, X.-H. N. In Vivo Imaging of Transport and Biocompatibility of Single Silver Nanoparticles in Early Development of Zebrafish Embryos. *ACS Nano* **2007,** 1, 133–143.

[22] Ahamed, M.; Karns, M.; Goodson, M.; Rowe, J.; Hussain, S. M.; Schlager, J. J.; Hong, Y. DNA damage response to different surface chemistry of silver nanoparticles in mammalian cells. *Toxicol. Appl. Pharmacol.* **2008,** 233, 404–410.

[23] Jia, C.-J.; Schüth, F. Colloidal metal nanoparticles as a component of designed catalyst. *Phys. Chem. Chem. Phys.* **2011,** 13, 2457–2487.

[24] Kraynov, A., Mueller, T. E. edited by Handy, S. Applications of Ionic Liquids in Science and Technology*:* Concepts for the Stabilization of Metal Nanoparticles in Ionic Liquids; *InTech,* **2011.**

[25] Liu, Y.; Zhang, Y.; Wang, J. Mesocrystals as a class of multifunctional materials. *CrystEngComm* **2014,** 16, 5948–5967.

[26] Faure, B.; Salazar-Alvarez, G.; Ahniyaz, A.; Villaluenga, I.; Berriozabal, G.; Miguel, Y. R. de; Bergström, L. Dispersion and surface functionalization of oxide nanoparticles for transparent photocatalytic and UV-protecting coatings and sunscreens. *Sci. Technol. Adv. Mater.* **2013,** 14, 1–23.

[27] Brar, S. K.; Verma, M. Measurement of nanoparticles by light-scattering techniques. *Trends Anal. Chem.* **2011,** 30, 4–17.

[28] Filipe, V.; Hawe, A.; Jiskoot, W. Critical evaluation of Nanoparticle Tracking Analysis (NTA) by NanoSight for the measurement of nanoparticles and protein aggregates. *Pharm. Res.* **2010,** 27, 796–810.

[29] Carr, B.; Wright, M. Nanoparticle Tracking Analysis*:* A Review of Applications and Usage 2010 - 2012; *NanoSight Ltd,* **2013.**

[30] Williams, D. B.; Carter, C. B. Transmission Electron Microscopy*:* A Textbook for Materials Science, 2nd ed.; *Springer US,* **2009.**

[31] Carney, R. P.; Kim, J. Y.; Qian, H.; Jin, R.; Mehenni, H.; Stellacci, F.; Bakr, O. M. Determination of nanoparticle size distribution together with density or molecular weight by 2D analytical ultracentrifugation. *Nat. Commun.* **2011,** 2, 1–8.

[32] Mitrano, D. M.; Barber, A.; Bednar, A.; Westerhoff, P.; Higgins, C.P.; Ranville, J. F. Silver nanoparticle characterization using single particle ICP-MS (SP-ICP-MS) and asymmetrical flow field flow fractionation ICP-MS (AF4-ICP-MS). *J. Anal. At. Spectrom.* **2012,** 27, 1131–1142.

[33] Ulrich, A.; Losert, S.; Bendixen, N.; Al-Kattan, A.; Hagendorfer, H.; Nowack, B.; Adlhart, C.; Ebert, J.; Lattuada, M.; Hungerbühler, K. Critical aspects of sample handling for direct nanoparticle analysis and analytical challenges using asymmetric field flow fractionation in a multi-detector approach. *J. Anal. At. Spectrom.* **2012,** 27, 1120–1130.

[34] Laborda, F.; Jiménez-Lamana, J.; Bolea, E.; Castillo, J. R. Selective identification, characterization and determination of dissolved silver(i) and silver

nanoparticles based on single particle detection by inductively coupled plasma mass spectrometry. *J. Anal. At. Spectrom.* **2011,** 26, 1362–1371.

[35] http://www.postnova.com/, (accessed Jul 16, 2015).

[36] Geiss, O.; Cascio, C.; Gilliland, D.; Franchini, F.; Barrero-Moreno, J. Size and mass determination of silver nanoparticles in an aqueous matrix using asymmetric flow field flow fractionation coupled to inductively coupled plasma mass spectrometer and ultraviolet-visible detectors. *J. Chromatogr. A* **2013,** 1321, 100–108.

[37] Hoque, M. E.; Khosravi, K.; Newman, K.; Metcalfe, C. D. Detection and characterization of silver nanoparticles in aqueous matrices using asymmetric-flow field flow fractionation with inductively coupled plasma mass spectrometry. *J. Chromatogr. A* **2012,** 1233, 109–115.

[38] Cascio, C.; Gilliland, D.; Rossi, F.; Calzolai, L.; Contado, C. Critical experimental evaluation of key methods to detect, size and quantify nanoparticulate silver. *Anal. Chem.* **2014,** 86, 12143–12151.

[39] Soto-Alvaredo, J.; Montes-Bayón, M.; Bettmer, J. Speciation of Silver Nanoparticles and Silver(I) by Reversed-Phase Liquid Chromatography Coupled to ICPMS. *Anal. Chem.* **2013,** 85, 1316–1321.

[40] Paleologos, E. K.; Giokas, D. L.; Karayannis, M. I. Micelle-mediated separation and cloud-point extraction. *Trends Anal. Chem.* **2005,** 24, 426–436.

[41] Watanabe, H. A non-ionic surfactant as a new solvent for liquid—liquid extraction of zinc(II) with 1-(2-pyridylazo)-2-naphthol. *Talanta* **1978,** 25, 585–589.

[42] Chao, J.-B.; Liu, J.-F.; Yu, S.-J.; Feng, Y.-D.; Tan, Z.-Q.; Liu, R.; Yin, Y.-G. Speciation Analysis of Silver Nanoparticles and Silver Ions in Antibacterial Products and Environmental Waters via Cloud Point Extraction-Based Separation. *Anal. Chem.* **2011,** 83, 6875–6882.

[43] Striegel, A. M. Hydrodynamic chromatography: packed columns, multiple detectors, and microcapillaries. *Anal. Bioanal. Chem.* **2012,** 402, 77–81.

[44] Tiede, K.; Boxall, A. B. A.; Tiede, D.; Tear, S. P.; David, H.; Lewis, J. A robust size-characterisation methodology for studying nanoparticle behaviour in 'real' environmental samples, using hydrodynamic chromatography coupled to ICP-MS. *J. Anal. At. Spectrom.* **2009,** 24, 964–972.

[45] Lewis, D. J. Hydrodynamic chromatography - inductively coupled plasma mass spectrometry, with post-column injection capability for simultaneous determination of nanoparticle size, mass concentration and particle number concentration (HDC-PCi-ICP-MS). *Analyst* **2015,** 140, 1624–1628.

[46] Trefry, J. C.; Monahan, J. L.; Weaver, K. M.; Meyerhoefer, A. J.; Markopolous, M. M.; Arnold, Z. S.; Wooley, D. P.; Pavel, I. E. Size selection and concentration of silver nanoparticles by tangential flow ultrafiltration for SERS-based biosensors. *J. Am. Chem. Soc.* **2010,** 132, 10970–10972.

[47] Snyder, L. R.; Kirkland, J. J.; Dolan, J. W. Introduction to Modern Liquid Chromatography, 3rd ed.; *Wiley,* **2010.**

[48] Dement'eva, O. V.; Mal'kovskii, A. V.; Filippenko, M. A.; Rudoy, V. M. Comparative study of the properties of silver hydrosols prepared by "citrate" and "citrate-sulfate" procedures. *Colloid J.* **2008,** 70, 561–573.

[49] Malina, D.; Sobczak-Kupiec, A.; Wzorek, Z.; Kowalski, Z. Silver nanoparticles synthesis with different concentrations of polyvinylpyrrolidone. *Dig. J. Nanomater. Bios.* **2012,** 7, 1527–1534.

[50] Sui, Z.; Chen, X.; Wang, L.; Xu, L.; Zhuang, W.; Chai, Y.; Yang, C. J. Capping effect of CTAB on positively charged Ag nanoparticles. *Physica E* **2006,** 33, 308–314.

[51] Behrens, S. H.; Grier, D. G. The charge of glass and silica surfaces. *J. Chem. Phys.* **2001,** 115, 6716–6721.

[52] Chakraborty, M.; Hsiao, F.-W.; Naskar, B.; Chang, C.-H.; Panda, A. K. Surfactant-Assisted Synthesis and Characterization of Stable Silver Bromide Nanoparticles in Aqueous Media. *Langmuir* **2012,** 28, 7282–7290.

[53] Liu, Y.; Tourbin, M.; Lachaize, S.; Guiraud, P. Silica nanoparticles separation from water: aggregation by cetyltrimethylammonium bromide (CTAB). *Chemosphere* **2013,** 92, 681–687.

[54] Tanaka, M.; Takahashi, Y.; Yamaguchi, N.; Kim, K.-W.; Zheng, G.; Sakamitsu, M. The difference of diffusion coefficients in water for arsenic compounds at various pH and its dominant factors implied by molecular simulations. *Geochim. Cosmochim. Acta* **2013,** 105, 360–371.

[55] Nightingale Jr., E. R. Phenomenological theory of ion solvation. *J. Phys. Chem.* **1959,** 63, 1381–1387.

[56] Bjerrum, J. On the tendency of the metal ions toward complex formation. *Chem. Rev.* **1950,** 46, 381–401.

[57] http://www.separations.us.tosohbioscience.com/ServiceSupport/TechSupport/ResourceCenter/FAQs/HPLCColumns/SizeExclusion/, (accessed Jul 29, 2015).

[58] Wang, Z.; Hattendorf, B.; Günther, D. Analyte response in laser ablation inductively coupled plasma mass spectrometry. *J. Am. Soc. Mass Spectrom.* **2006,** 17, 641–651.